Transcriptome of the GSH-Depleted Lens Reveals Changes in Detoxification and EMT Signaling Genes, Transport Systems, and Lipid Homeostasis

Jeremy A. Whitson,[1] Xiang Zhang,[2] Mario Medvedovic,[2] Jenny Chen,[2] Zongbo Wei,[1] Vincent M. Monnier,[1,3] and Xingjun Fan[1]

[1]Department of Pathology, Case Western Reserve University, Cleveland, Ohio, United States
[2]Department of Environmental Health, University of Cincinnati, Cincinnati, Ohio, United States
[3]Department of Biochemistry, Case Western Reserve University, Cleveland, Ohio, United States

Correspondence: Xingjun Fan, Case Western Reserve University, Department of Pathology, 2301 Cornell Road, Cleveland, OH 44106, USA; xxf3@case.edu.
Vincent M. Monnier, Case Western Reserve University, Department of Pathology, 2301 Cornell Road, Cleveland, OH 44106, USA; vmm3@case.edu.

Submitted: December 29, 2016
Accepted: April 13, 2017

Citation: Whitson JA, Zhang X, Medvedovic M, et al. Transcriptome of the GSH-depleted lens reveals changes in detoxification and EMT signaling genes, transport systems, and lipid homeostasis. *Invest Ophthalmol Vis Sci*. 2017;58:2666–2684. DOI: 10.1167/iovs.16-21398

Purpose. To understand the effects of glutathione (GSH)-deficiency on genetic processes that regulate lens homeostasis and prevent cataractogenesis.

Methods. The transcriptome of lens epithelia and fiber cells was obtained from C57BL/6 LEGSKO (lens GSH-synthesis knockout) and buthionine sulfoximine (BSO)-treated LEGSKO mice and compared to C57BL/6 wild-type mice using RNA-Seq. Transcriptomic data were confirmed by qPCR and Western blot/ELISA on a subset of genes.

Results. RNA-Seq results were in excellent agreement with qPCR (correlation coefficients 0.87–0.94 and $P < 5E\text{-}6$ for a subset of 36 mRNAs). Of 24,415 transcripts mapped to the mouse genome, 441 genes showed significantly modulated expression. Pathway analysis indicated major changes in epithelial-mesenchymal transition (EMT) signaling, visual cycle, small molecule biochemistry, and lipid metabolism. GSH-deficient lenses showed upregulation of detoxification genes, including *Aldh1a1, Aldh3a1* (aldehyde dehydrogenases), *Mt1, Mt2* (metallothioneins), *Ces1g* (carboxylesterase), and *Slc14a1* (urea transporter UT-B). Genes in canonical EMT pathways, including *Wnt10a*, showed upregulation in lens epithelia samples. Severely GSH-deficient lens epithelia showed downregulation of vision-related genes (including crystallins). The BSO-treated LEGSKO lens epithelia transcriptome has significant correlation ($r = 0.63$, $P < 0.005$) to that of lens epithelia undergoing EMT. Protein expression data correlated with transcriptomic data and confirmed EMT signaling activation.

Conclusions. These results show that GSH-deficiency in the lens leads to expression of detoxifying genes and activation of EMT signaling, in addition to changes in transport systems and lipid homeostasis. These data provide insight into the adaptation and consequences of GSH-deficiency in the lens and suggest that GSH plays an important role in lenticular EMT pathology.

Keywords: LEGSKO mouse, cataract, glutathione, oxidative stress, epithelial mesenchymal transition, RNA-seq, gene expression

Age-related cataract is a multifactorial disease associated with the accumulation of posttranslational modifications (PTMs) on lens proteins.[1] These PTMs may lead to the formation of insoluble aggregates, which scatter light and reduce visual acuity. The versatile antioxidant glutathione (GSH) is present at millimolar levels within the lens and helps to prevent the formation of damaging PTMs on lens protein.[2] It has been demonstrated that lenticular GSH content decreases significantly with advanced age, particularly in the lens nucleus, which is thought to result from a decrease in GSH synthesis in the metabolically active lens cortex[3] and a growing barrier around the lens nucleus that prevents its diffusion from the lens cortex.[4] This progressive loss of GSH may play an important role in age-related cataractogenesis by producing an environment wherein lens proteins are more susceptible to the PTMs that result in their insolubility and aggregation.

In order to better study the role of GSH in the lens and its relation to cataract, the lens glutathione synthesis knockout (LEGSKO) mouse model was generated.[5] These mice were developed using a lox/Cre system that knocks out GCLC, the first step in GSH synthesis, specifically within the lens. As a result, these mice show reduced lens GSH content and develop opacities that mimic human age-related cataract. However, severe opacities do not develop until >9 months of age and, with subsequent generations, these mice show a further delayed onset of cataractogenesis.

Based on these results, we set out to determine how mouse lenses adapt to GSH-deficiency and maintain the integrity of their lens protein. This question was partially addressed by the discovery that mouse eyes have >1 mM GSH in their vitreous humor and that the lens and vitreous humor GSH pools equilibrate via passive diffusion when the lens becomes deficient in GSH.[6] The vitreous humor GSH pool is derived from circulating GSH and can be depleted by treating mice with the systemic GSH synthesis inhibitor buthionine sulfoximine (BSO), which leads to the further depletion of LEGSKO lens

GSH.[6] We demonstrated in the same study that humans and other large animal eyes lack this vitreous GSH reservoir,[6] which may be one aspect of why species such as humans and canines appear to be more susceptible to cataract formation than rodents.[7] Large mammals like humans may be especially reliant on the activity of other gene products to maintain a reduced and toxin-free environment in the aging lens when the lenticular GSH pool diminishes.

In this study, we set out to determine the gene expression changes that occur in the lens in response to GSH-depletion in order to better understand the adaptations and consequences of GSH-depletion in the lens.

Methods

Animal Work

Both the LEGSKO and wild-type (WT) mice used in this study were of C57BL/6 genetic background and age-matched at 6 months. Groups used for all experiments were as follows: four male WT mice, four male LEGSKO mice, and four male LEGSKO mice exclusively receiving drinking water containing 10 mM BSO for 1 month prior to sample collection. Mice were housed under diurnal lighting conditions and allowed free access to food and water. All animals were used in accordance with the guidelines of the Association for Research in Vision and Ophthalmology for the Use of Animals in Ophthalmology and Vision Research, and experimental protocols for this study were approved by the Institutional Animal Care and Use Committee (IACUC) of Case Western Reserve University.

Sample Preparation

Eyes were removed from mice following CO_2 asphyxiation and washed with RNAlater solution (Thermo Fisher Scientific, Waltham, MA, USA). Lenses were carefully removed by cutting away cornea and sclera and were washed in ice-cold nuclease-free water. Lens epithelial cells were isolated by removing the lens capsule with forceps and removing any visible fiber cells adherent to the capsule. Cortical lens fiber cells were isolated from the remaining fiber cell mass using forceps. Samples of the same tissue from both eyes of each mouse were pooled together in 1 mL RNAlater solution. Samples were kept at 4°C overnight and then frozen at −80°C until RNA extraction.

RNA-Seq

RNA-Seq was performed in quadruplicate samples by the Genomics, Epigenomics and Sequencing Core (GESC) in the University of Cincinnati as described below.

Sample tissue was homogenized in 0.4 to 0.8 mL Lysis/Binding Buffer from the mirVana miRNA Isolation Kit (Thermo Fisher Scientific) using a Precellys 24 homogenizer (Bertin Corp., Rockville, MD, USA). Total RNA extraction was performed according to the mirVana protocol, and the RNA was eluted with 100 µL elution buffer. Quality of RNA was assessed using a 2100 Bioanalyzer (Agilent Technologies, Santa Clara, CA, USA).

NEBNext Poly(A) mRNA Magnetic Isolation Module (New England BioLabs, Ipswich, MA, USA) was used for initial poly(A) RNA purification with a total of 1 µg good quality total RNA as input. An Apollo 324 system (WaferGen, Fremont, CA, USA) was then used with PrepX PolyA Isolation Kit (WaferGen) for automated poly(A) RNA isolation.

NEBNext Ultra Directional RNA Library Prep Kit (New England BioLabs) was used for library preparation, which uses dUTP in cDNA synthesis to maintain strand specificity. In short, the isolated poly(A) RNA was Mg^{2+}/heat fragmented to ~200 bp, reverse transcribed to first strand cDNA, followed by second strand cDNA synthesis labelled with dUTP. The purified cDNA was end repaired and dA tailed, and then ligated to an adapter with a stem-loop structure. The dUTP-labelled second strand cDNA was removed by USER enzyme to maintain strand specificity. After indexing via PCR (~12 cycles) enrichment, the amplified library was cleaned up by AMPure XP beads for QC analysis.

To check the quality and yield of the purified library, 1 µL of the library was analyzed by Bioanalyzer (Agilent Technologies) using a DNA high sensitivity chip. To accurately quantify the library concentration for the clustering, the library was $1:10^4$ diluted in dilution buffer (10 mM Tris-HCl, pH 8.0 with 0.05% Tween 20), and measured by qPCR using the Kapa Library Quantification Kit (Kapabiosystem, Woburn, MA, USA) with ABI's 9700HT real-time PCR system (Thermo Fisher Scientific).

Cluster Generation and HiSeq Sequencing

To study differential gene expression, individually indexed and compatible libraries were proportionally pooled (~25 million reads per sample in general) for clustering in cBot System (Illumina, San Diego, CA, USA). Libraries at the final concentration of 15 pM were clustered onto a single read (SR) flow cell using Illumina TruSeq SR Cluster Kit v3, and sequenced for 50 bp using the TruSeq SBS Kit on an Illumina HiSeq system.

Bioinformatic Analysis

To analyze differential gene expression, sequence reads were aligned to the mouse genome using standard Illumina sequence analysis pipeline, which was analyzed by The Laboratory for Statistical Genomics and Systems Biology at the University of Cincinnati. The report consists of the following: (1) RNA-seq data, QC, and sample clustering analyzing results; (2) all gene expression level in RNA samples, normalized as read per kilobase of transcript per million mapped reads (RPKM); and (3) significantly differentially expressed genes between groups with $P < 0.05$ and false-discovery rate (FDR) < 0.1.

Validation of RNA-Seq Data by Real Time PCR (qPCR)

An independent group of 6-month-old male C57Bl/6 mice of the same genotype/treatment used in RNA-Seq were used for qPCR confirmation of RNA-Seq results. Lens epithelia and cortical fiber cells were dissected in ice-cold nuclease-free water and pooled together from both eyes of each mouse. Samples were immediately frozen in liquid nitrogen. RNA was extracted and purified using a standard Trizol protocol (Thermo Fisher Scientific). RNA purity and concentration was analyzed using a Nanodrop 2000c and only samples showing a 260:280 ratio of $\geq$1.8 and a 260:230 ratio of $\geq$2.0 were used (Thermo Fisher Scientific). One microgram of fiber cell RNA and at least 200 ng of epithelia RNA were treated with amplification grade DNase I (Thermo Fisher Scientific), for each sample, to remove genomic DNA. RNA was converted to cDNA using M-MuLV Reverse Transcriptase and murine RNase inhibitor (New England BioLabs). An equal mixture of oligo(dT) and random oligo primers were used at a concentration of 20 µM for the synthesis.

Primers for qPCR were predesigned KicqStart primers ordered from Sigma-Aldrich Corp. (St. Louis, MO, USA), with the exception of primers for *Mt1* and *Aldh1a7*, which were designed using Primer-BLAST software (National Center for

Investigative Ophthalmology & Visual Science

Biotechnology Information, Bethesda, MD, USA). Primers were verified by performing qPCR in triplicate on WT C57BL/6 mouse whole lens cDNA at three different concentrations and with a no-template control in order to determine reproducibility and linearity of amplification. Specificity of primers was determined based on the presence of a single peak in melt curve analysis. All primer data are reported (Supplementary Fig. S2).

Hprt and *Rer1* were used in tandem as reference genes for relative quantification of expression (ΔΔCt method) using KicqStart SYBR Green Master Mix with ROX (Sigma-Aldrich Corp.). Five, fifteen, or thirty nanograms of lens epithelia or fiber cell RNA was used for each reaction, based on the established linear range of amplification for each primer. Standard cycling was used with an initial 10-minute hold at 95°C followed by 40 cycles of 95°C for 15 seconds and 60°C for 1 minute.

Western Blots

Eyes and lenses were dissected in ice-cold 50 mM HEPES, 150 mM NaCl, and pH 7.4 buffer. Lens epithelial and cortical fiber cells were separated and pooled from both eyes of each mouse and then homogenized in ice-cold lysis buffer (50 mM Tris-HCl, 1 mM PMSF, 0.5% Triton-X).

Based on Pierce BCA Assay (Thermo Fisher Scientific) results, 15 μg lens epithelia extracts and 30 μg lens cortical fiber extracts were separated on 12% SDS-PAGE gels. Protein was transferred to 0.45 μm polyvinylidene fluoride (PVDF) membranes using standard transfer buffer (25 mM Tris, 190 mM glycine, 20% methanol, pH 8.3) by running at 100 V for 1 hour. Blocking was performed with 5% milk in Tris-buffered saline with tween-20 (TBS-T).

The following primary antibodies and dilutions were used: mouse monoclonal anti-metallothionein (MT; UC1MT, Thermo Fisher Scientific) 1:1000, mouse polyclonal anti-GSTK1 (ab155407, Abcam, Cambridge, MA, USA) 1:2000, rabbit polyclonal anti-TNC (ab19011, EMD Millipore, Temecula, CA, USA) 1:1000, rabbit monoclonal anti-LAMB3 (EPR7525, Abcam) 1:1000, mouse monoclonal anti-GAPDH (MA5-15738, Thermo Fisher Scientific) 1:5000, and rabbit polyclonal anti-Type I collagen (ab34710, Abcam) 1:2000.

Secondary horseradish peroxidase-linked anti-mouse (7076S, Cell Signaling Technology, Danvers, MA, USA) and anti-rabbit (7074S, Cell Signaling Technology) antibodies were used at a 1:5000 dilution.

WNT10A ELISA

Quantification of Wnt Family Member 10A (WNT10A) in the aqueous humor of mice was performed by drawing aqueous humor from the anterior chamber of mouse eyes using a 10-μL Nanofil syringe (World Precision Instruments, Sarasota, FL, USA) equipped with a 30-gauge needle. Aqueous humor was pooled from both eyes of each mouse. WNT10A protein content was assessed using a commercially available ELISA kit (OKEH03519, Aviva Systems Biology, San Diego, CA, USA) following the manufacturer's instructions. Aqueous humor samples were diluted 1:20 in sample diluent buffer, and all samples and standards were run in duplicate.

Immunofluorescent Imaging of α-Smooth Muscle Actin (α-SMA)

Whole mouse lenses were stained with FITC-labeled mouse monoclonal α-SMA antibody (F3777, Sigma-Aldrich Corp.) at a 1:1000 dilution. Images were taken using a Leica SP8 gSTED confocal microscope equipped with two 3 Hyd SP GaAsP detectors and AOBS system lasers. The 488-nm green fluorescence was obtained using the same settings for all samples, and the cell nucleus was labeled by 4′,6-diamidino-2-phenylindole (DAPI).

Statistical Analysis

All values are expressed as mean ± standard deviations (SDs) with $n = 4$. Only P values < 0.05 were considered statistically significant. P values for correlations were derived from the Pearson correlation coefficient (r) using the equation $t = r\sqrt{[(1-r^2)/(N-2)]}$ and determining the corresponding two-tailed P value.

RESULTS

Overview of Significant Gene Expression Changes Resulting From GSH Depletion in the Lens

RNA-Seq data from lens epithelia and fiber cells were successfully mapped to 15,997 and 14,475 genes, respectively. Six thousand fifty-seven of the mapped genes overlap between the two data sets, resulting in a total expression database of 24,415 genes. All samples of the same cell type had a high correlation coefficient (>0.986) without any clear outliers (Supplementary Figs. S1A, S1B). A total of 441 genes showed significantly (>2-fold, $P < 0.05$, FDR < 0.1) modulated gene expression (Fig. 1A). Fifty-four genes were significantly upregulated in LEGSKO epithelia, while 38 were downregulated. LEGSKO fiber cells had 84 genes upregulated and 60 downregulated genes. The results were more dramatic in LEGSKO lenses treated with BSO, with the epithelia having 78 upregulated genes and 37 downregulated genes, and the fiber cells have 125 upregulated genes and 97 downregulated genes.

These gene changes were sorted into major pathways of metabolism (Fig. 1B), transcription (normally referred to as gene expression but changed here to avoid confusion; Fig. 1C), cell cycle (Fig. 1D), immunity (Fig. 1E), developmental biology (Fig. 1F), transport of small molecules (Fig. 1G), extracellular matrix (ECM) organization (Fig. 1H), protein metabolism (Fig. 1I), and cellular stress response (Fig. 1J) by Reactome software (reactome.org, provided in the public domain). Metabolism, transcription, and cell cycle were the most robustly altered pathways while, surprisingly, cellular stress response was the least affected pathway.

RPKM values, fold changes, and significance measurements are listed for all significant gene expression changes with >2-fold in the Supplementary Data. Significant changes are highlighted in red and green for upregulated and downregulated genes, respectively. Specific gene changes in major biological pathways are shown in Supplementary Figures S3 through S12. Raw and processed data sets can also be accessed at the NCBI Gene Expression Omnibus (Ascension ID: GSE95688).

RNA-Seq Data Shows Strong Differential Expression of Lens Epithelia and Fiber Cell Marker Genes and Excellent Agreement With qPCR Results

Based on the work of the Robinson laboratory[8] pointing to the existence of region specific gene expression in the lens, we validated our protocol by determining the expression of established lens epithelia and fiber cell marker genes (Figs. 2A, 2B). For all marker genes, expression was much greater in

Investigative Ophthalmology & Visual Science

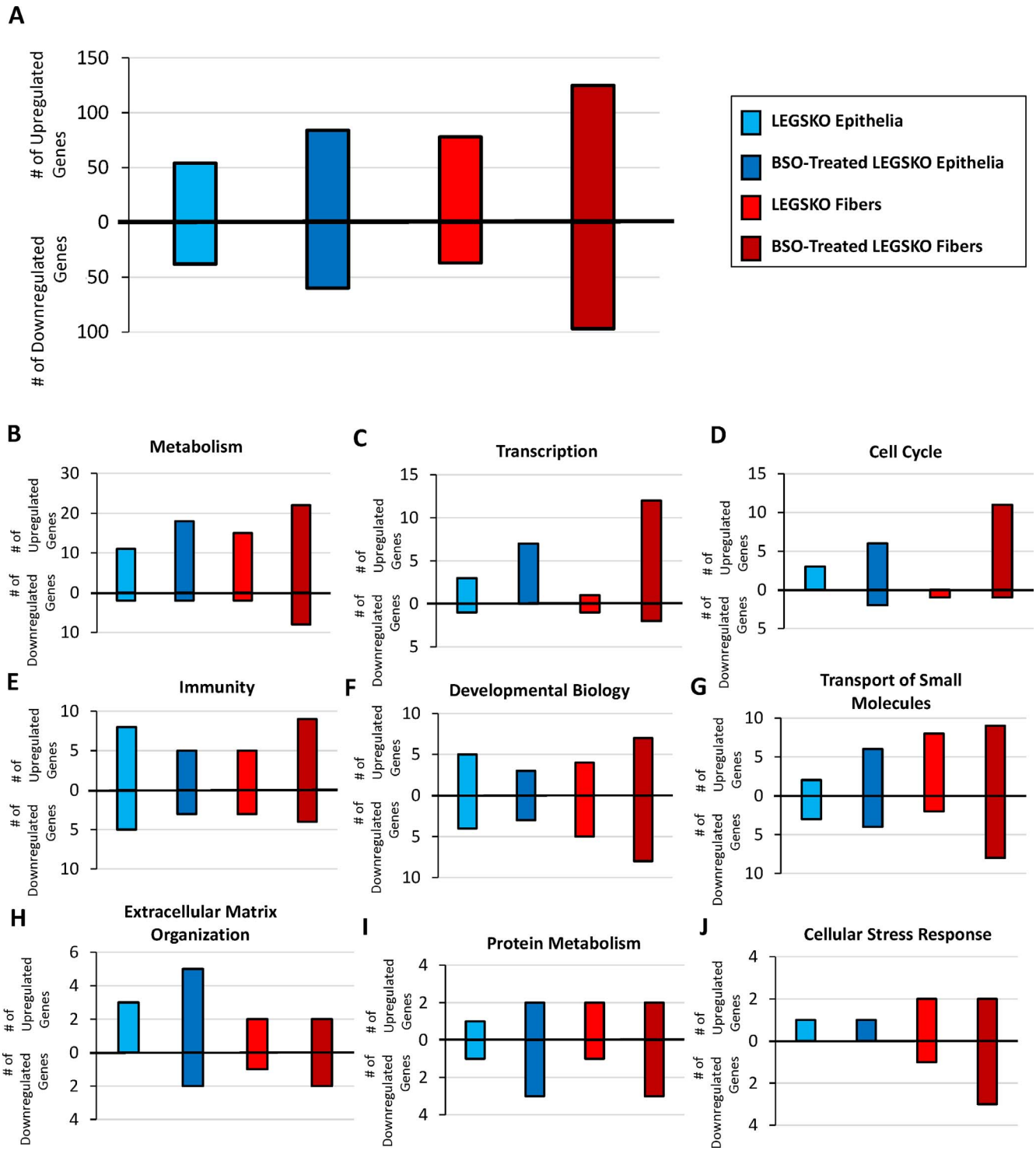

Figure 1. Overview of significant gene expression changes. (**A**) Total number of significantly (minimum 2-fold regulation change, $P < 0.05$, FDR < 0.1) up- and downregulated genes for each group compared to WT. (**B**–**J**) Number of significantly up- and downregulated genes (relative to WT control) in major biological pathways of (**B**) metabolism, (**C**) transcription, (**D**) cell cycle, (**E**) immunity, (**F**) developmental biology, (**G**) transport of small molecules, (**H**) ECM organization, (**I**) protein metabolism, and (**J**) cellular stress response.

the appropriate lens tissue, indicating successful isolation of lens epithelia and fiber cell compartments.

RNA-Seq results were validated by performing qPCR on a subset of transcripts (Figs. 2C–J). cDNA was obtained from the lens epithelia and fiber cells of independent but identical groups of mice. A total of 36 transcripts were tested, which were chosen from among the most robustly significantly up- and downregulated genes, as well as unchanged genes with a high baseline expression in the lens. At least 16 transcripts were analyzed for each group. In all cases, the qPCR results were highly consistent with RNA-Seq results, with Pearson correlation coefficients ranging from 0.87 to 0.94 and $P < 5E\text{-}6$.

Investigative Ophthalmology & Visual Science

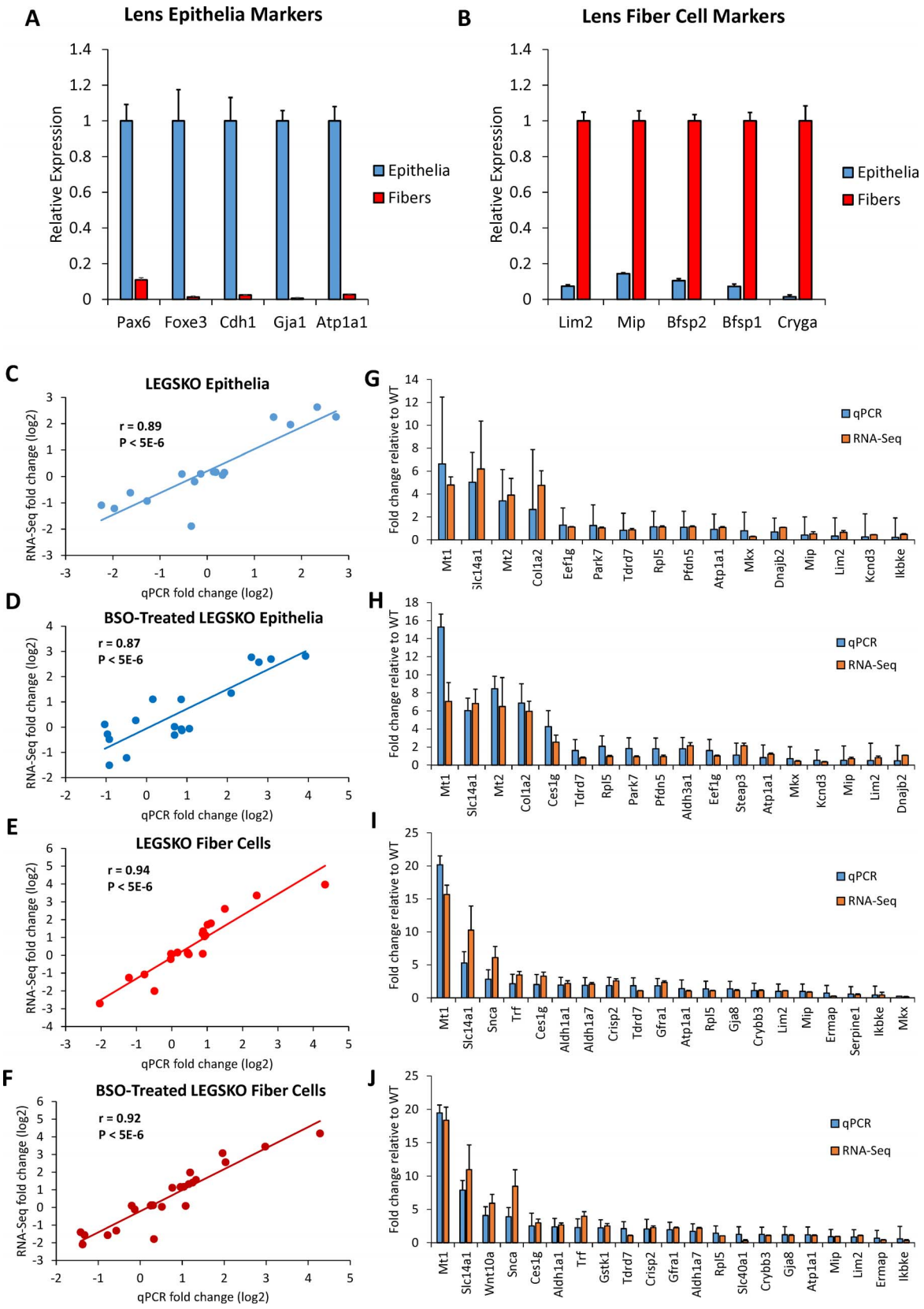

Figure 2. Verification of RNA-Seq results. (**A**, **B**) Differential expression of (**A**) lens epithelium and (**B**) fiber cell marker genes. Expression shown as relative fold changes based on means with SDs from WT RPKM RNA-Seq values. (**C**–**F**) Confirmation of RNA-Seq results by RT-qPCR. Each point represents one gene. (**C**) LEGSKO lens epithelia. (**D**) BSO-treated LEGSKO lens epithelia. (**E**) LEGSKO lens fiber cells. (**F**) BSO-treated LEGSKO lens fiber cells. Values are log2 converted means of relative fold change. (**G**–**J**) Direct comparison of RNA-Seq and qPCR results for each gene tested. Values in bar graphs are means of relative fold changes ± SD. $n = 4$.

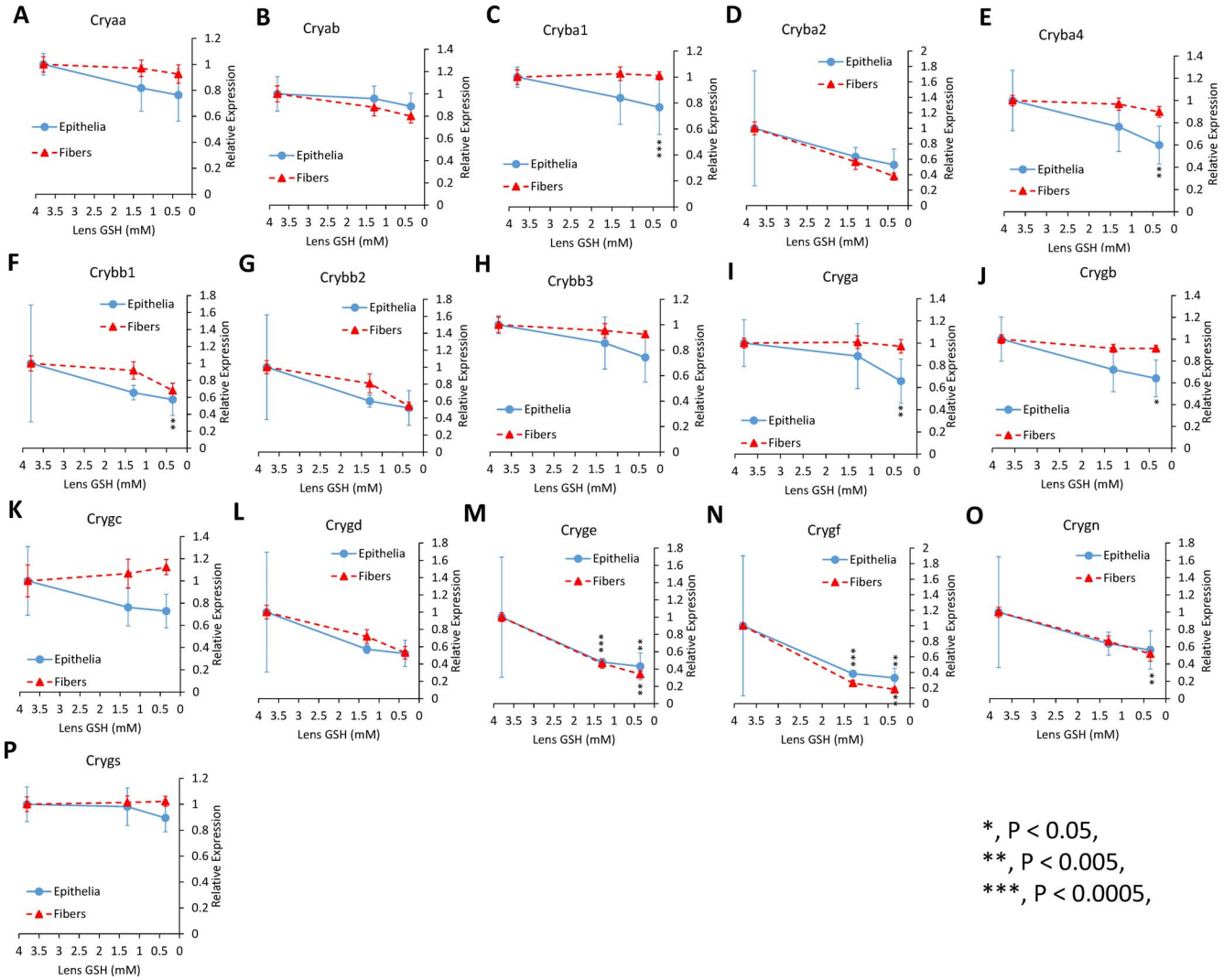

FIGURE 3. Crystallin gene expression by GSH content of WT, LEGSKO, and BSO-treated LEGSKO lenses. (**A**) *Cryaa*, (**B**) *Cryab*, (**C**) *Cryba1*, (**D**) *Cryba2*, (**E**) *Cryba4*, (**F**) *Crybb1*, (**G**) *Crybb2*, (**H**) *Crybb3*, (**I**) *Cryga*, (**J**) *Crygb*, (**K**) *Crygc*, (**L**) *Crygd*, (**M**) *Cryge*, (**N**) *Crygf*, (**O**) *Crygn*, and (**P**) *Crygs*. Values are mean ± SD; 3.8 mM GSH = WT; 1.3 mM GSH = LEGSKO; 0.35 mM GSH = BSO-treated LEGSKO. Fold change and significance is relative to WT.

These results confirm the veracity and reproducibility of the transcriptome.

GSH Depletion Results in a Partial Downregulation of β- and γ-Crystallins

Because crystallins are essential to the function of the lens, any transcriptional changes may have a major effect on cataractogenesis, and the expression of all crystallin genes was examined. LEGSKO lens epithelia showed a slight trend of decrease in all crystallin transcripts and this difference was more exaggerated in BSO-treated epithelia (Fig. 3). However, only downregulation of *Cryge* (Fig. 3M) and *Crygf* (Fig. 3O) reached significance ($P < 0.05$, FDR < 0.1) in LEGSKO epithelia, while downregulation of *Cryba1* (Fig. 3C), *Cryba4* (Fig. 3E), *Crybb1* (Fig. 3F), *Cryge* (Fig. 3M), and *Crygf* (Fig. 3N) was significant ($P < 0.05$, FDR < 0.1) in BSO-treated LEGSKO epithelia. In either case, only changes in *Cryge* and *Crygf* reached a 2-fold threshold.

Lens fiber cells did not show the same general downregulation of crystallin genes and only had significant ($P < 0.05$, FDR < 0.1) decreases in BSO-treated LEGSKO lens fiber cells, where *Cryga* (Fig. 3I), *Crygb* (Fig. 3J), *Cryge* (Fig. 3M), *Crygf* (Fig. 3N), and *Crygn* (Fig. 3O) were significantly downregulated. Of these, *Cryga*, *Cryge*, and *Crygf* had a >2-fold downregulation.

Trends Identified in Upstream Regulators and Molecular/Cellular Functions of Genes With Modulated Expression

The major upstream regulators of the lens' transcriptomic response to GSH depletion were determined using Ingenuity Pathway Analysis (IPA) Software (QIAgen, Hilden, Germany) (Table 1). This analysis provides information on pathways, and their upstream regulators, involved in the gene expression changes within GSH-deficient lenses.

LEGSKO lens epithelia showed responses regulated upstream by transforming growth factor β1 (TGF-β1), tumor necrosis factor (TNF), low-density lipoprotein (LDL), AE binding protein 1 (AEBP1), and peroxisome proliferator-activated receptor γ (PPARG). Based on the IPA analysis readout, TGF-β1, TNF, AEBP1, and PPARG all play roles in

Table 1. Top Upstream Regulators and Molecular and Cellular Functions of Gene Expression Changes in GSH-Deficient Lenses

LEGSKO Epithelia	BSO-Treated LEGSKO Epithelia	LEGSKO Fiber Cells	BSO-Treated LEGSKO Fiber Cells
Upstream regulators (*P* value)			
AEBP1 (7.13E-08)	CRX (1.23E-12)	RHO (1.17E-05)	RARA (6.97E-06)
TGF-β1 (1.19E-07)	OTX2 (1.67E-10)	PPARG (2.60E-05)	TNF (2.44E-05)
TNF (1.51E-07)	RHO (1.60E-09)	TNF (4.13E-05)	SMARCA4 (3.05E-05)
PPARG (7.36E-07)	AEBP1 (1.67E-09)	Sos (9.10E-05)	EP300 (4.10E-05)
LDL (1.01E-06)	p53 (1.80E-07)	IL-1B (1.48E-04)	IL-1B (4.85E-05)
Molecular and cellular functions (*P* value range)			
Cell death and survival (3.80E-03 – 3.72E-07)	Cell morphology (8.47E-03 – 1.18E-10)	Energy production (7.17E-03 – 5.92E-06)	Cellular assembly and organization (8.50E-03 – 1.92E-12)
Cellular development (3.80E-03 – 6.79E-07)	Cellular compromise (5.28E-03 – 1.76E-08)	Lipid metabolism (9.15E-03 – 5.92E-06)	DNA replication, recombination, and repair (4.16E-04 – 1.92E-12)
Cellular growth and proliferation (3.80E-03 – 6.79E-07)	Cellular development (8.47E-03 – 2.61E-06)	Small molecule biochemistry (9.35E-03 – 5.92E-06)	Posttranslational modification (3.68E-10 – 3.25E-12)
Lipid metabolism (3.80E-03 – 2.12E-06)	Cellular growth and proliferation (6.21E-03 – 2.61E-06)	Vitamin and mineral metabolism (8.05E-03 – 5.92E-06)	Protein synthesis (6.20E-03 – 3.25E-12)
Small molecule biochemistry (3.80E-03 – 2.12E-06)	Posttranslational modification (7.66E-03 – 3.07E-06)	Drug metabolism (4.85E-03 – 1.84E-05)	Cellular function and maintenance (8.61E-03 – 1.93E-06)

proliferation, epithelial-mesenchymal transition (EMT), and epithelial cancers, while LDL, AEBP1, and PPARG are all indicated to regulate lipid homeostasis.

The top upstream regulators of BSO-treated LEGSKO lens epithelia were AEBP1, the tumor suppressor p53, cone-rod homeobox protein (CRX), rhodopsin (RHO), and orthodenticle homeobox 2 (OTX2). p53 is a major tumor suppressor and a regulator of EMT.[9] IPA indicates that CRX, RHO, and OTX2 regulate the visual cycle and eye development and are associated with vision defects.

Similar results were found in LEGSKO fiber cells, where the primary regulators were RHO, PPARG, TNF, son of sevenless homolog (Sos), and interleukin 1β (IL-1β). Sos and IL-1β are also noted EMT regulators.

The major regulators of the response in BSO-treated LEGSKO fibers were TNF, IL-1β, retinoic acid receptor α (RARA), SWI/SNF related, matrix associated, actin dependent regulator of chromatin, subfamily a, member 4 (SMARCA4), and E1A binding protein p30 (EP300). IPA reports all of these molecules as regulators of cell growth/survival and epithelial cancers.

IPA software was also used to determine the most common molecular and cellular functions of the differentially regulated genes for each group (Table 1). The most common functions found in the LEGSKO lens epithelia genetic response matched well with the upstream regulators that were noted and had a particular emphasis on cellular integrity. These functions include cell death and survival, cellular development, cellular growth and proliferation, lipid metabolism, and small molecule biochemistry.

BSO-treated LEGSKO lens epithelia showed similar functions, with the major ones being cell morphology, cellular compromise, cellular development, cellular growth and proliferation, and posttranslational modification (relating to oxidation and tetramerization of proteins).

The response in LEGSKO lens fiber cells showed functions that were more metabolically focused, with categories of energy production, lipid metabolism, small molecule biochemistry, vitamin and mineral metabolism, and drug metabolism showing significant changes.

BSO-treated LEGSKO lens fiber cells showed different major functions of cellular assembly and organization, DNA replication, recombination, and repair, PTM, protein synthesis, and cellular function and maintenance. The difference between the treated and untreated LEGSKO fibers could imply a more robust stress response in the BSO treated animal.

Expression of Several Detoxification Genes Is Inversely Related to Decreasing Lenticular GSH Content

Because a loss of GSH is expected to result in increased oxidative stress and a decreased clearance of toxic species in the lens, such as 4-hydroxynonenal and H_2O_2, regulation changes in genes relating to detoxification was expected and investigated as a function of decreasing GSH content, with ~3.8 mM in WT lenses, ~1.3 mM in LEGSKO lenses, and ~0.35 mM in BSO-treated LEGSKO lenses (Fig. 4).

Both epithelia and fiber cells showed changes in aldehyde dehydrogenase genes, with *Aldh1l1* (Fig. 4E) and *Aldh3a1* (Fig. 4F) having >2-fold upregulation in BSO-treated LEGSKO epithelia ($P < 0.0005$) and *Aldh1a7* (Fig. 4D) and *Aldh1a1* (Fig. 4B) showing a similar upregulation in both LEGSKO and BSO-treated LEGSKO fiber cells ($P < 0.0005$). Both fiber cell groups also showed ~3-fold downregulation of *Aldh1a3* (Fig. 4C; $P < 5E\text{-}8$), the only significantly downregulated gene in this category for either tissue.

Both epithelia and fiber cell groups also showed upregulation of the essential detoxification gene *Ces1g* (Fig. 4H; $P < 0.05$), which encodes liver carboxylesterase, *Slc14a1* (Fig. 4L; $P < 5E\text{-}12$), which encodes the urea transporter UT-B, and *Mt1* (Fig. 4J; $P < 5E\text{-}15$), which encodes the metal chelator/antioxidant metallothionein 1.

Mt1 had a particularly robust upregulation, with a 4- to 7-fold increase in epithelia and >15-fold upregulation in fiber cells across both GSH-deficient groups. Epithelia showed a similar upregulation of metallothionein 2 (*Mt2*; Fig. 4K; $P < 5E\text{-}8$), which is nearly identical in sequence to *Mt1*. *Mt2* was not upregulated in GSH-deficient fiber cells.

Additionally, untreated LEGSKO lens epithelia showed >2-fold upregulation of aldo-keto reductase family member B10 (*Akr1b10*; Fig. 4A; $P < 0.0005$). Both fiber cell groups showed >2-fold upregulation of arsenite (3+) methyltransferase (*As3mt*; Fig. 4G; $P < 5E\text{-}5$). Glutathione S-transferase κ 1 (*Gstk1*) was upregulated in BSO-treated LEGSKO lens fiber cells (Fig. 4I; $P < 0.005$).

Several Transport Systems Are Modulated as a Function of Decreasing Lenticular GSH Content

The top 10 most robust changes in the category of small molecule transport are shown in Figure 5. These changes

Investigative Ophthalmology & Visual Science

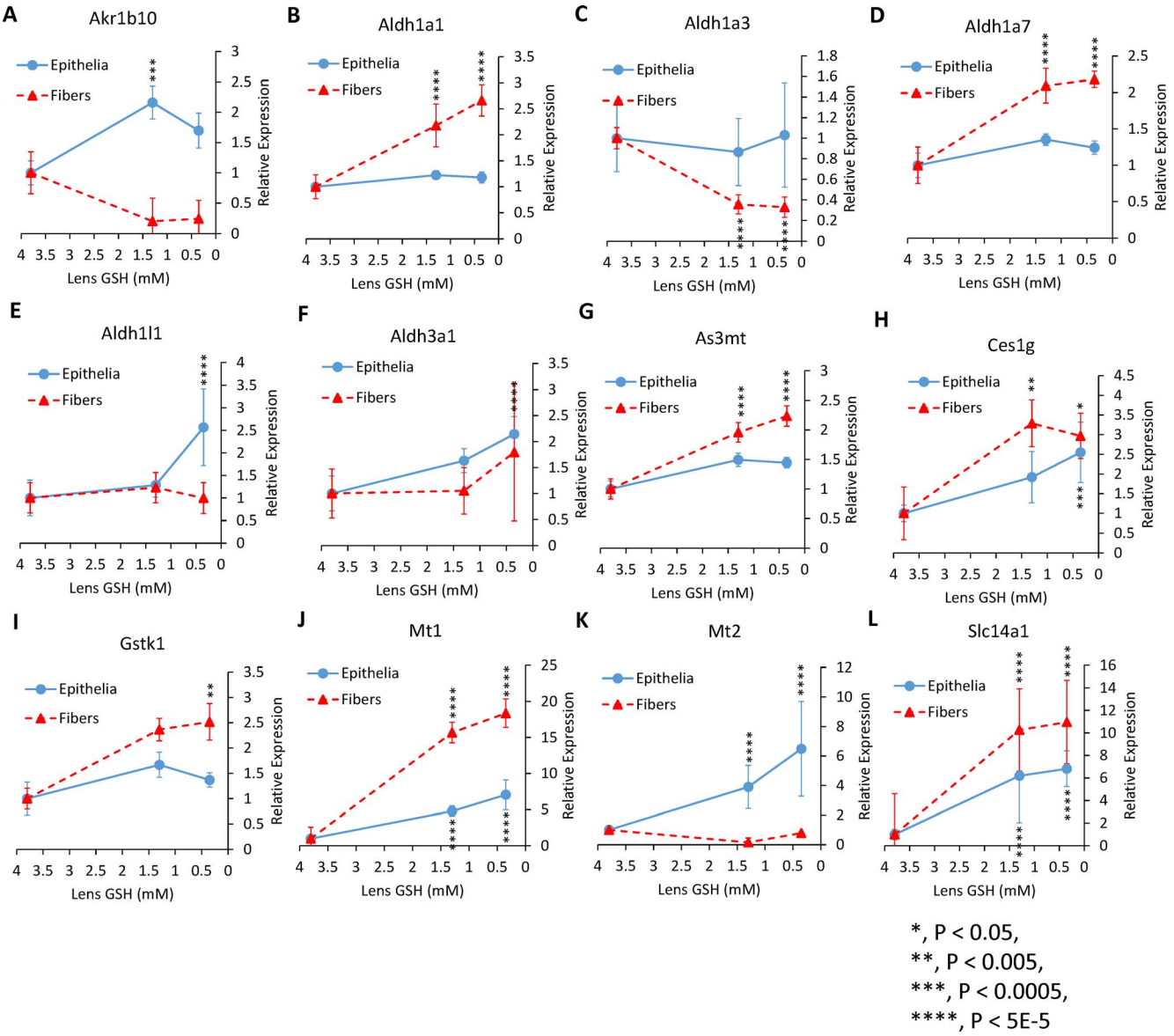

Figure 4. Expression changes in detoxification genes by GSH content of WT, LEGSKO, and BSO-treated LEGSKO lenses. (**A**) *Akr1b10*, (**B**) *Aldh1a1*, (**C**) *Aldh1a3*, (**D**) *Aldh1a7*, (**E**) *Aldh1l1*, (**F**) *Aldh3a1*, (**G**) *As3mt*, (**H**) *Ces1g*, (**I**) *Gstk1*, (**J**) *Mt1*, (**K**) *Mt2*, (**L**) *Slc14a1*. Values are mean ± SD; 3.8 mM GSH = WT; 1.3 mM GSH = LEGSKO; 0.35 mM GSH = BSO-treated LEGSKO. Fold change and significance are relative to WT.

include 5.2-fold upregulation of the connexin gene, *Gjb3* (Fig. 5C), which encodes Cx31, in BSO-treated LEGSKO epithelia ($P < 0.005$). Cx31 has not been previously characterized to be expressed within the lens.

Potassium channel gene *Kcnd1* (Fig. 5F), which could play a potential role in lens microcirculation, showed a >2-fold downregulation in both epithelia and fiber cells ($P < 0.005$). The expression of this gene showed a strong positive correlation with lens GSH content in both tissue compartments.

Several changes were seen in iron transport genes, including 6.0- to 8.5-fold upregulation of α-synuclein (*Snca*; Fig. 5I; $P <$ 5E-9), which has been recently characterized as a ferrireductase,[10] and 3- to 4-fold upregulation of transferrin (*Trf*; Fig. 5J; $P <$ 5E-13) expression in fiber cells. These changes track well with lens GSH content and imply enhanced uptake of iron by GSH-deficient lens fiber cells.

Expression changes were noted in multiple γ-aminobutyric acid receptors, with *Gabrr1* being 6-fold upregulated (Fig. 5D; $P < 0.005$) and *Gabrr2* being 2- and 5-fold downregulated (Fig. 5E; $P < 0.005$) in LEGSKO and BSO-treated LEGSKO fiber cells, respectively.

κ casein (*Csn3*), a transmembrane regulator without a well-defined role in the lens, was 14.4-fold upregulated in BSO-treated LEGSKO epithelia (Fig. 5B; $P < 0.0005$), but not in the untreated mouse, and was not expressed at all in fiber cells.

Expression changes were found in multiple lipid transport genes. Fatty acid transporter gene *Slc27a6* was 5.5-fold upregulated in BSO-treated LEGSKO epithelia (Fig. 5H; $P <$ 0.0005) and there was a 9- to 13-fold upregulation of the cholesterol and phospholipid adenosine triphosphate (ATP)-binding cassette transporter gene *Abcg1* in fiber cells (Fig. 5A; $P <$ 1E-8). These regulation changes imply a potentially enhanced uptake of lipids and membrane composition changes.

Investigative Ophthalmology & Visual Science

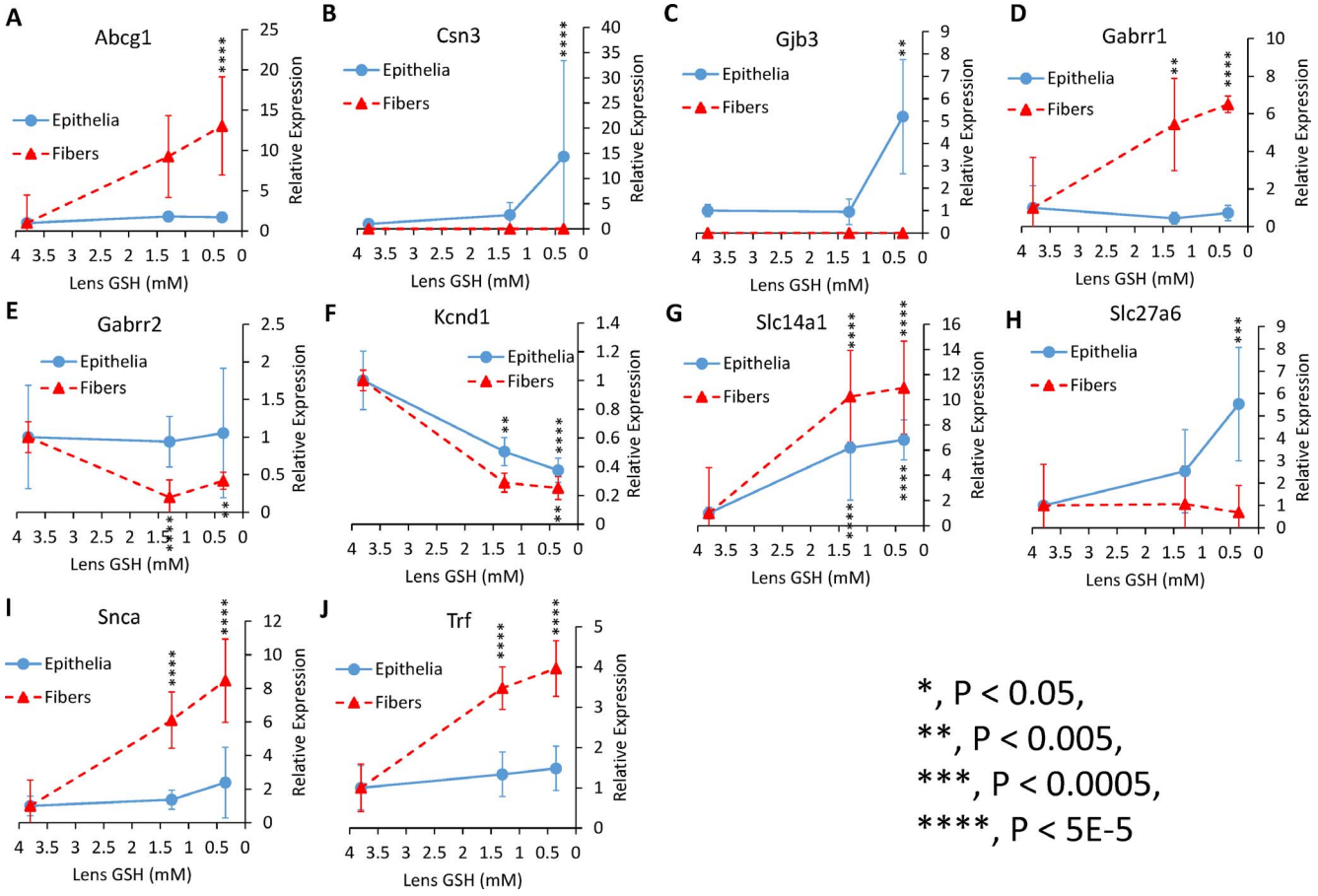

FIGURE 5. Top 10 expression changes in small molecule transport genes by GSH content of WT, LEGSKO, and BSO-treated LEGSKO lenses. (**A**) *Abcg1*, (**B**) *Csn3*, (**C**) *Gjb3*, (**D**) *Gabrr1*, (**E**) *Gabrr2*, (**F**) *Kcnd1*, (**G**) *Slc14a1*, (**H**) *Slc27a6*, (**I**) *Snca*, (**J**) *Trf*. Values are means ± SD; 3.8 mM GSH = WT; 1.3 mM GSH = LEGSKO; 0.35 mM GSH = BSO-treated LEGSKO. Fold change and significance are relative to WT.

An Array of Lipid Metabolism Genes Show Modulated Expression as a Function of Decreasing Lenticular GSH Content

Many other lipid metabolism gene expression changes occurred, and the top 10 most robust of these changes are shown in Figure 6. An additional ATP-binding cassette lipid transporter, *Abca13,* was 4.5-fold upregulated in BSO-treated LEGSKO fiber cells (Fig. 6A; $P < 0.05$). LEGSKO lens epithelia showed an 8.7-fold downregulation of the membrane trafficking gene copine-6 (*Cpne6*; Fig. 6D; $P < 0.005$). This transcript was not present in lens fiber cells and does not have a well-defined role in the lens.

Several changes were noted in genes involved in the breakdown of lipids. All samples showed a 2.5- to 5.4-fold upregulation of the lipase inhibitor gene G0/G1 switch 2 (*G0s2*; Fig. 6H; $P < 5E\text{-}5$). Cytochrome P450, family 2, subfamily j, polypeptide 9 (*Cyp2j9),* which is an oxidoreductase involved in cholesterol and steroid metabolism, was 8.0- to 10.7-fold upregulated in fiber cells (Fig. 6E; $P < 5E\text{-}7$). Dimethylglycine dehydrogenase (*Dmgdh),* which catabolizes the phospholipid head group component choline, was 18.1-fold upregulated in BSO-treated LEGSKO fiber cells (Fig. 6F; $P < 0.005$).

Four and a half LIM domains 2 (*Fhl2*) was 5.7-fold downregulated in BSO-treated LEGSKO fiber cells (Fig. 6G; $P < 5E\text{-}5$). *Fhl2* is thought to play a role in the development of extracellular membranes, and its downregulation is associated with cellular transformation.[11]

Gal encodes galanin, a neuroendocrine peptide that plays a role in dietary behavior, and was 6.3-fold upregulated in BSO-treated LEGSKO epithelia (Fig. 6I; $P < 0.0005$). Although upregulation of galanin is associated with increased consumption of dietary fats,[12] and thus lipid balance, it is unclear why a neuroendocrine peptide would be expressed in the lens and what effect it has. Similarly, the circadian metabolism-regulating gene *Npas2*, which encodes the transcription factor neuronal PAS domain-containing protein 2, was 5.8-fold downregulated in BSO-treated LEGSKO epithelia (Fig. 6J; $P < 0.0005$), but the effect on the lens is unclear.

Lens GSH Depletion Induces Gene Expression Changes Related to EMT Pathways

Based on the identification of TGF-β and TNF as primary upstream regulators of the gene expression changes found in GSH-deficient epithelium (Table 1), activation of EMT signaling in lens epithelium was investigated. A number of changes were found in genes associated with canonical EMT pathways (Figs. 7A–J).

Constant between the LEGSKO and BSO-treated LEGSKO epithelia was robust upregulation of Wnt family member 10A (*Wnt10a*), with a >20-fold increase in expression in both sample groups compared to WT (Fig. 7J; $P < 5E\text{-}5$).

Additionally, LEGSKO lens epithelium showed a slightly over 2-fold upregulation of EMT signaling initiators, including epidermal growth factor (*Egf*; Fig. 7A; $P < 5E\text{-}5$), fibroblast growth factor 4 (*Fgfr*; Fig. 7B; $P < 0.005$), and *IL-1B* (Fig. 7D; P

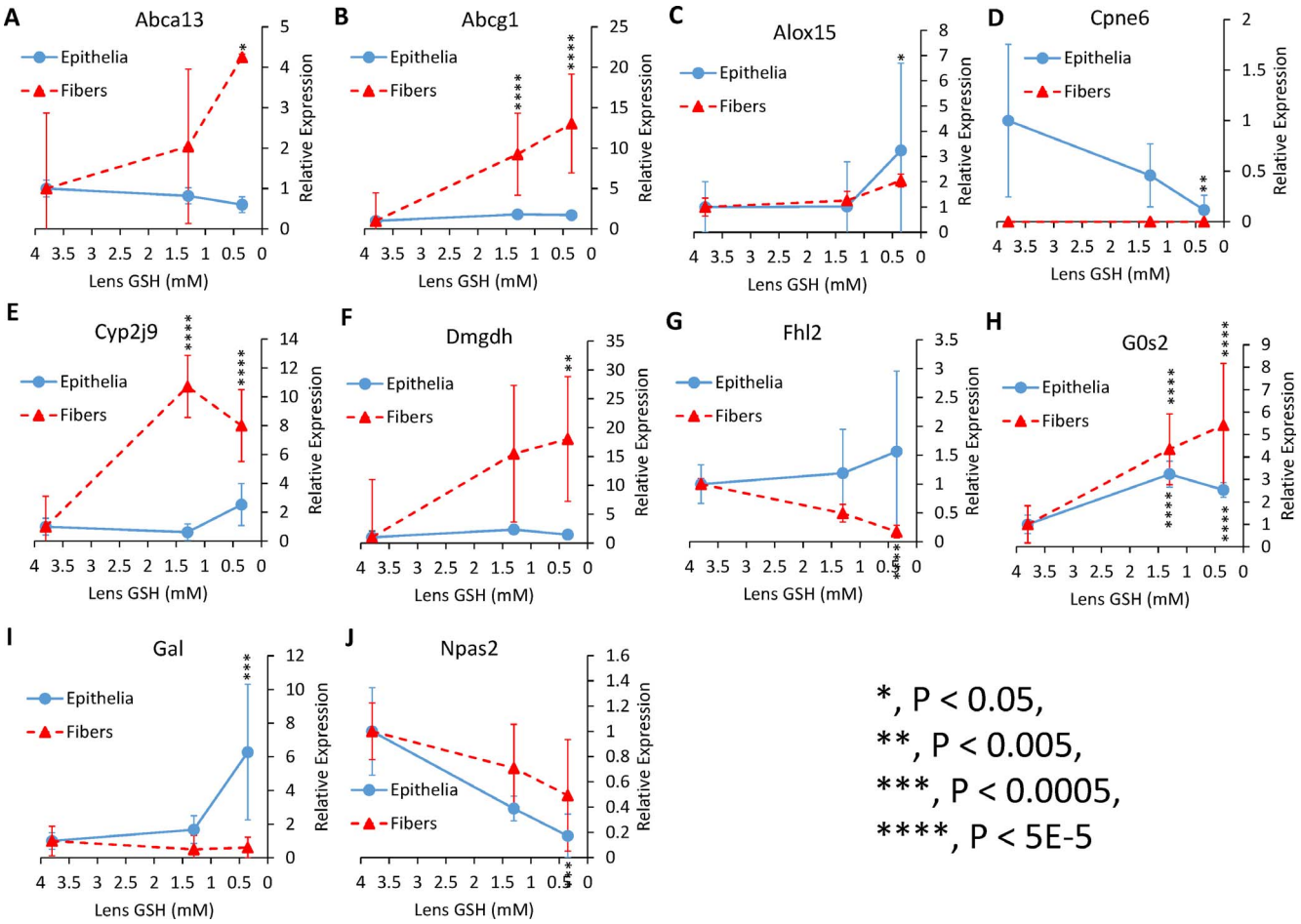

Figure 6. Top 10 expression changes in lipid metabolism genes by GSH content of WT, LEGSKO, and BSO-treated LEGSKO lenses. (**A**) *Abca13*, (**B**) *Abcg1*, (**C**) *Alox15*, (**D**) *Cpne6*, (**E**) *Cyp2j9*, (**F**) *Dmgdh*, (**G**) *Fhl2*, (**H**) *G0s2*, (**I**) *Gal*, (**J**) *Npas2*. Values are mean ± SD; 3.8 mM GSH = WT; 1.3 mM GSH = LEGSKO; 0.35 mM GSH = BSO-treated LEGSKO. Fold change and significance are relative to WT.

< 0.0005), as well as downstream regulator ras homolog family member h (*Rhoh*; Fig. 7F; $P < 1E\text{-}9$) and a robust 5.9-fold upregulation of downstream regulator spleen associated tyrosine kinase (*Syk*; Fig. 7H; $P < 0.005$). LEGSKO lenses also showed a 3.8-fold downregulation of nuclear receptor subfamily 4 group member 1 (*Nr4a1*; Fig. 7E; $P < 5E\text{-}5$), an inhibitor of TGF-β signaling.

BSO-treated LEGSKO epithelium did not recapitulate all of these findings; instead showing a 3.8-fold upregulation of TGF, β-induced (*Tgfbi*; Fig. 7I; $P < 5E\text{-}5$) and a 2.3-fold upregulation of immediate early response 3 (*Ier3*; Fig. 7C; $P < 0.005$), both of which are more tangentially related to EMT pathways. Secreted phosphoprotein 1 (*Spp1*), which inhibits *Akt* signaling, was 9.3-fold upregulated (Fig. 7G; $P < 1E\text{-}5$). The differences between the treated and untreated mice could indicate that most of these proteins are only minor contributors to EMT in the lens, while WNT10A is the major driver, or that BSO-treated and untreated LEGSKO epithelia are in different stages of the EMT process, with the untreated cells being in the initiating stages and the treated cells being at a more terminal/transformed stage.

EMT signaling in the lens is expected to result in a loss of lens/eye marker genes, so expression of noncrystallin genes related to vision and the eye were investigated in lens epithelia (Figs. 7K–T). While expression of vision genes showed a general trend of downregulation in LEGSKO epithelia, these changes did not reach significance. However, these changes were more robust in BSO-treated LEGSKO epithelia, which showed a broad downregulation of genes involved in visual transduction with fold changes ranging from 3 to 20 ($P < 0.005$). All of these genes are strongly expressed in the eye and play a role in vision but do not have a known function within the lens.

A number of genes associated with cell cycle progression showed significant regulation changes (Figs. 7U–C2). Six genes encoding histone subunits showed 2- to 3-fold upregulation in epithelia samples when compared to WT (Figs. 7V–A2; $P < 0.005$), indicating active cellular proliferation. The DNA repair gene *Dmc1* showed a 5.2-fold increase in BSO-treated LEGSKO epithelia (Fig. 7U; $P < 0.005$), while tubulin genes showed >2-fold downregulation (Figs. 7B2, 7C2; $P < 0.005$).

ECM organization gene changes were investigated, since EMT is associated with fibrotic changes involving ECM (Figs. 7D2–K2). Type I collagen expression increases with EMT, and *Col1a1* and *Col1a2* are commonly used markers of EMT signaling.[13] Interestingly, *Col1a1* was 2.4-fold downregulated in BSO-treated LEGSKO epithelia (Fig. 7E2; $P < 0.005$), while *Col1a2* was 4.8- and 6-fold upregulated in untreated and BSO-treated LEGSKO epithelia, respectively (Fig. 7F2; $P < 5E\text{-}5$). However, given that the RPKM values of *Col1a2* were much greater than the RPKM values of *Col1a1* in lens epithelia (Supplementary Data), it is likely that the expression changes in *Col1a2* are much more significant and have a larger effect on the actual protein level.

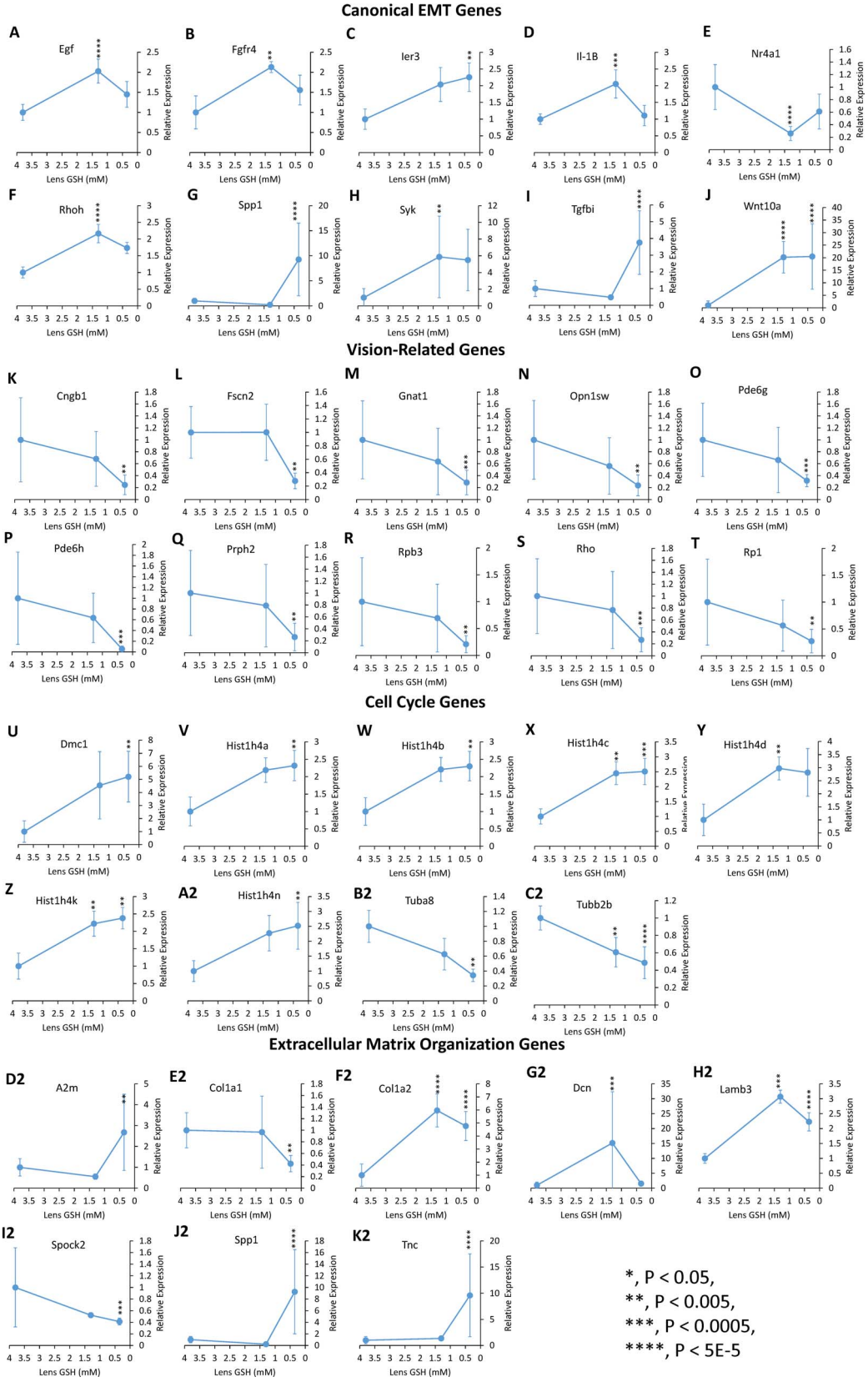

Figure 7. Top expression changes in pathways related to EMT in lens epithelia by GSH content of WT, LEGSKO, and BSO-treated LEGSKO lenses. (**A–J**) Lens epithelium expression changes in canonical EMT pathway genes. (**A**) *Egf*, (**B**) *Fgfr4,* (**C**) *Ier3*, (**D**) *Il-1B*, (**E**) *Nr4a1*, (**F**) *Rhoh*, (**G**) *Spp1*, (**H**) *Syk*, (**I**) *Tgfbi*, (**J**) *Wnt10a*. (**K–T**) Top 10 lens epithelia expression changes in noncrystallin vision genes. (**K**) *Cngb1*, (**L**) *Fscn2*, (**M**) *Gnat1*, (**N**) *Opn1sw*, (**O**) *Pde6g*, (**P**) *Pde6h*, (**Q**) *Prph2*, (**R**) *Rpb3*, (**S**) *Rho*, (**T**) *Rp1*. (**U–C2**) Lens epithelia expression changes in cell cycle genes. (**U**) *Dmc1*, (**V**) *Hist1h4a*, (**W**) *Hist1h4b*, (**X**) *Hist1h4c*, (**Y**) *Hist1h4d*, (**Z**) *Hist1h4k*, (**A2**) *Hist1h4n*, (**B2**) *Tuba8*, (**C2**) *Tubb2b*. (**D2–K2**) Lens epithelia expression changes in ECM organization genes. (**D2**) *A2M*, (**E2**) *Col1a1*, (**F2**) *Col1a2*, (**G2**) *Dcn*, (**H2**) *Lamb3*, (**I2**) *Spock2*, (**J2**) *Spp1*, (**K2**) *Tnc*. Values are mean ± SD; 3.8 mM GSH = WT; 1.3 mM GSH = LEGSKO; 0.35 mM GSH = BSO-treated LEGSKO. Fold change and significance are relative to WT.

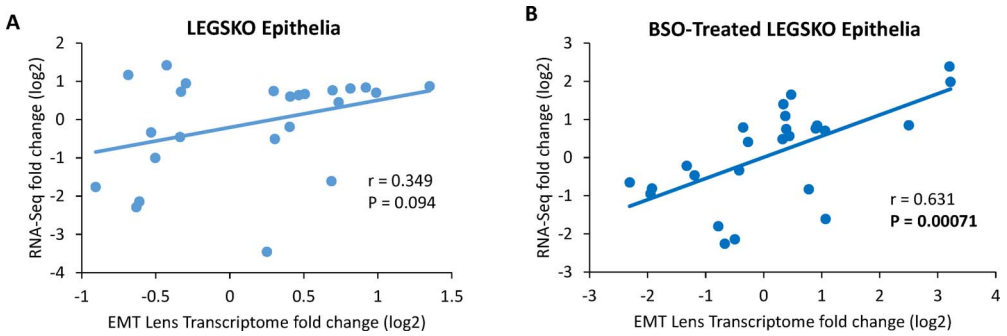

Figure 8. Correlation of the GSH-deficient mouse lens transcriptome with an EMT model transcriptome. (**A**) Correlation of model to LEGSKO lens epithelia. (**B**) Correlation of model to BSO-treated LEGSKO lens epithelia. EMT model transcriptome data taken, with permission, from an independent study.[18] Values are log2 converted means of relative fold-changes. Each point represents one gene.

Laminin subunit β 3 (*Lamb3*), a component of lens capsules,[14] was >2-fold upregulated in epithelia samples (Fig. 7H2; $P < 0.0001$). *Tnc* encodes tenascin C, an ECM protein associated with wound healing[15] and was 9.6-fold upregulated in BSO-treated LEGSKO epithelia (Fig. 7K2; $P <$ 5E-5). *Dcn* encodes decorin, an extracellular protease that interacts with TGF-β[16] and was 15.2-fold upregulated in untreated LEGSKO epithelia (Fig. 7G2; $P < 0.0005$). *Spock2* encodes an ECM protein with similarity to SPARC/osteonectin, an essential protein for lens clarity[17] and was 2.4-fold downregulated in BSO-treated LEGSKO epithelia (Fig. 7I2; $P < 0.0005$).

To determine whether the transcriptional profile of GSH-deficient lens epithelium is similar to the transcriptional profile of a lens EMT model, transcriptomic data from this study were compared to transcriptomic data from a study by Medvedovic et al.[18] in which gene expression was measured in C57BL/6 mouse lens epithelia after removal of lens fiber cells. It was found that lens epithelia underwent EMT 1 week postsurgery and began to differentiate into fiber cells at later time points.[18] This 1-week postsurgery expression data were used as a genetically similar EMT model and correlated to GSH-deficient lens epithelia expression data by comparing all genes that show significant ($P < 0.05$, FDR < 0.1) regulation changes in both studies, regardless of fold change. From this comparison, it was determined that LEGSKO lens epithelia trend toward a positive correlation with EMT lenses, but this correlation does not reach significance ($r = 0.353$, $P = 0.0906$; Fig. 8A), whereas BSO-treated LEGSKO lens epithelia show a robust positive correlation with epithelia from EMT lenses ($r = 0.633$, $P < 0.001$; Fig. 8B). The specific overlapping gene changes that were compared are shown in Table 2, with changes occurring in the same direction bolded. These data indicate that, as lens GSH becomes increasingly deficient, lens epithelia increasingly develop EMT-like transcriptional profiles.

Protein Changes in GSH-Deficient Lenses Show Similarity to Transcriptional Changes and Confirm EMT Signaling Activation

To confirm that the transcriptional changes presented here result in similar protein changes, and that activation of EMT signaling is truly occurring in GSH-deficient lenses, the expression of selected proteins was analyzed in mouse lenses (Fig. 9).

GSTK1 was significantly ($P < 0.05$) upregulated in BSO-treated LEGSKO fiber cells but not untreated LEGSKO fiber cells (Fig. 9G), closely matching the transcriptional results (Fig. 3I). MT expression was tested in both lens epithelia and fiber cells using an antibody that does not distinguish between different forms of MT (Figs. 9B, 9H). Both tissues showed a trend of upregulation in the LEGSKO lens but surprising downregulation in the BSO-treated LEGSKO lens. This trend only reached significance ($P < 0.05$) in fiber cells, where it was much more pronounced, with MT being 4-fold upregulated in the LEGSKO fibers and undetectable in the BSO-treated LEGSKO fibers. Tenascin C (TNC), laminin β 3 (LAMB3), and type I collagen were significantly ($P < 0.05$) upregulated in BSO-treated LEGSKO epithelia but not untreated LEGSKO epithelia (Figs. 9C–E).

Because it is a secreted protein, WNT10A content of the aqueous humor, rather than the lens, was determined by ELISA (Fig. 9I). WNT10A expression was nearly 4-fold greater in LEGSKO aqueous humor compared to WT ($P < 0.05$) and nearly 10-fold greater in BSO-treated LEGSKO aqueous humor ($P < 0.05$).

Expression of alpha smooth muscle actin (α-SMA), a commonly used marker for EMT activation, was analyzed by immunofluorescent staining of WT and GSH-deficient LEGSKO lenses (Fig. 10). GSH-deficient lenses show a robust expression of α-SMA in nucleated regions of the lens, with the strongest signal being in the lens epithelia, that is absent in control lenses, indicating activation of EMT.

Discussion

While the impact of GSH depletion in the aging and cataractous human and mouse lens is widely understood in regards to oxidative PTMs,[19] its impact on gene expression is poorly understood. To date, no other transcriptomic studies on the topic of the GSH-depleted lens have been reported. The emerging question is how the observed transcriptomic changes should be interpreted, given that the LEGSKO mouse lens is a model of chronic adaption to GSH depletion from birth on, while BSO treatment induces more acute GSH depletion by inhibiting systemic GSH formation, and thus reducing the amount taken up by the lens.[6] Moreover, the lens epithelial layer is the major active site of gene expression in the lens, while nucleated cortical fiber cells have more limited transcription and translational capabilities.[8] Thus, in order to gain a clearer picture of the expression changes occurring, lenses were separated into distinct epithelial and cortical fiber regions before RNA or protein extraction and gene expression in both regions were analyzed. All of these aspects are important as context and should be considered when interpreting gene expression data from the GSH-deficient lens.

Investigative Ophthalmology & Visual Science

Table 2. Comparison of Overlapping Gene Expression Changes in GSH-Deficient and EMT Lens[18] Transcriptomes

Gene	Description	LEGSKO Lens Epithelia	BSO-Treated LEGSKO Lens Epithelia	EMT Lens Epithelia (Medvedovic et al., 2006)[18]
1110032A03Rik	RIKEN cDNA 1110032A03 gene	1.34		−1.14
Abcb1a	**ATP-binding cassette, subfamily B (MDR/TAP), member 1A**	**1.65**	**1.90**	**1.70**
Actg1	actin, γ, cytoplasmic 1		−1.18	1.33
Agrn	agrin	−1.24		1.66
Alas1	aminolevulinic acid synthase 1		−1.25	1.73
Aldh3a1	aldehyde dehydrogenase family 3, subfamily A1	1.63	2.15	−3.05
Apoe	**apolipoprotein E**	**2.03**	**2.13**	**1.63**
Ccl2	chemokine (C-C motif) ligand 2	−1.59		2.25
Cldn10	**claudin 10**	**−1.40**		**−2.00**
Crybb1	**crystallin, β B1**		**−1.56**	**−4.78**
Ctgf	**connective tissue growth factor**		**1.30**	**2.64**
Dbnl	**drebrin-like**	**−1.25**		**−1.37**
Fabp5	**fatty acid binding protein 5, epidermal**		**−1.69**	**−3.48**
Fscn2	**fascin homolog 2, actin-bundling protein, retinal**		**−3.60**	**−1.75**
Gosr2	golgi SNAP receptor complex member 2	1.26		−1.42
Gpnmb	**glycoprotein (transmembrane) nmb**		**5.85**	**1.80**
Hebp1	**heme binding protein 1**	**1.44**		**1.59**
Hexb	hexosaminidase B	−1.21		1.93
Hist1h2bc	**histone 1, H2bc**	**1.40**		**1.56**
Homer2	homer homolog 2 (Drosophila)		1.76	−1.78
Krt15	**keratin 15**	**2.58**		**1.83**
Lctl	**lactase-like**	**−1.51**	**−1.38**	**−4.41**
Ldlr	**low density lipoprotein receptor**	**−1.11**	**−1.31**	**−1.26**
Lim2	**lens intrinsic membrane protein 2**	**−1.53**		**−4.89**
Nfatc2	**nuclear factor of activated T-cells, cytoplasmic 2**	**−1.85**		**−3.39**
Oplah	**5-oxoprolinase (ATP-hydrolysing)**		**1.39**	**1.48**
Osmr	**oncostatin M receptor**		**1.42**	**3.14**
Pir	**pirin**	**1.79**		**1.76**
Rasgef1b	**GPI-GAMMA 4**		**−2.23**	**−1.38**
Rbp3	**retinol binding protein 3, interstitial**		**−4.81**	**−1.57**
Rho	**rhodopsin**		**−3.75**	**−1.93**
Sat1	**spermidine/spermine N1-acetyl transferase 1**	**1.25**	**1.34**	**1.68**
Serpina3n	**serine (or cysteine) proteinase inhibitor, clade A, member 3N**		**9.62**	**3.96**
Slc9a3r1	**solute carrier family 9 (sodium/hydrogen exchanger), isoform 3 regulator 1**	**1.69**		**1.37**
Slco2a1	**solute carrier organic anion transporter family, member 2a1**	**1.93**	**1.94**	**1.79**
Stab1	stabilin 1	−1.32		2.68
Stat5b	signal transducer and activator of transcription 5B	1.21		−10.98
Sulf1	**sulfatase 1**		**1.33**	**2.13**
Tcea3	**transcription elongation factor A (SII), 3**		**−2.44**	**−1.16**
Tln2	**talin 2**		**1.28**	**1.40**
Tnc	**tenascin C**		**9.59**	**5.24**
Tsc22d1	**TSC22 domain family, member 1**	**1.35**		**1.52**

Overlapping gene changes occurring in the same direction are shown in bold.

The GSH-Deficient Lens Transcriptome Shows an Unusual Oxidative Stress Response and Indicates Protective Detoxification Genes

While it was expected that depletion of GSH would result in enhanced expression of many genes regulated by the transcription factor Nrf2, the master regulator of the antioxidant response and GSH synthesis,[20] this response was much more muted than expected. Nrf2 did not emerge as a significant regulator of the observed transcriptional changes (Table 1) and the only Nrf2 regulated genes[20] that showed a change in expression were *Aldh3a1*, *Mt1*, and thioredoxin-interacting protein (*Txnip*; Supplementary Data). Interestingly, *Txnip*, which acts as a pro-oxidant by inhibiting thioredoxin activity, was slightly upregulated, even though binding of Nrf2 to the *Txnip* promoter suppresses its expression.[21] Additionally, there was a general lack of regulation changes in traditional antioxidant genes, such as peroxidases and superoxide dismutase.

It was expected that various GSH-utilizing enzymes would be upregulated in order to maintain a high rate of activity despite lower levels of GSH; however, this trend was not found, with one exception. The only GSH-related enzyme that was upregulated was *Gstk1*, which has not been shown to be regulated by Nrf2[22] and is only distantly related to other GSH S-transferase genes.[23] However, recent study of GSTK1 has

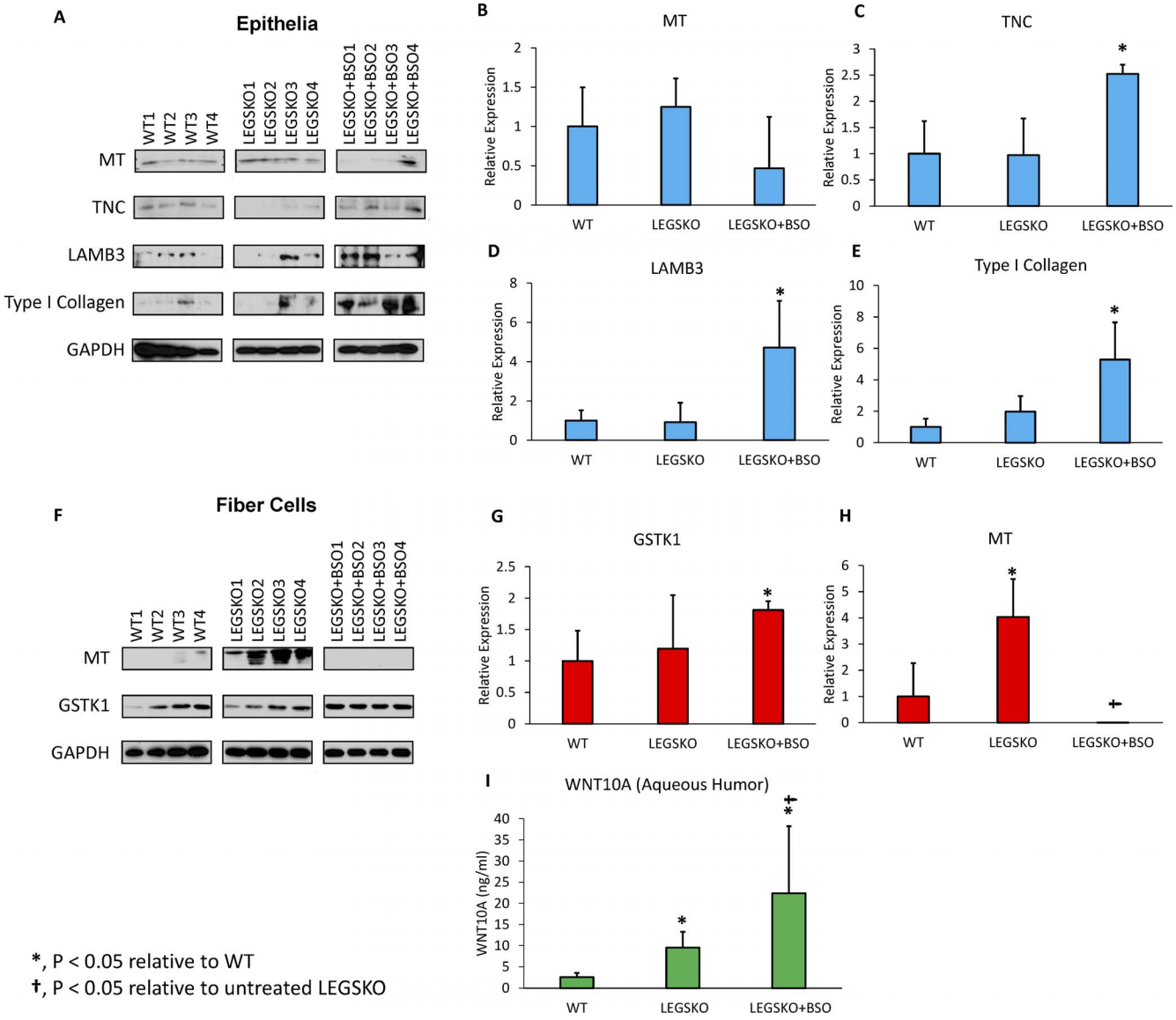

Figure 9. Analysis of GSH-deficient lens protein expression. (**A**) Western blots for MT, TNC, LAMB3, and type I collagen in WT, LEGSKO, and BSO-treated LEGSKO lens epithelia. GAPDH used as loading control. (**B–E**) Quantification of Western blots. Relative expression values are normalized to GAPDH. (**F**) Western blots for MT and GSTK1 in WT, LEGSKO, and BSO-treated LEGSKO lens cortical fiber cells. GAPDH used as loading control. (**G**, **H**) Quantification of Western blots in (**F**). Relative expression values are normalized to GAPDH. (**I**) Comparison of WNT10A levels in the aqueous humor of WT, LEGSKO, and BSO-treated LEGSKO eyes as determined by ELISA.

revealed that it shares a homologous thioredoxin-like domain with GSH peroxidase[24] and has putative peroxidase activity.[25] Since it was found that the upregulation of GSTK1 is carried through to the protein level (Fig. 9G), GSTK1 has strong potential for protecting the lens.

These results may indicate that the lens is unable to properly respond to GSH-deficiency and produce a typical oxidative stress response. This apparent lack of robust Nrf2 activation may help to explain why lenses develop GSH-deficiency in the first place, since a lack of GSH production should result in Nrf2 activation and, thus, expression of new GSH synthetic machinery to replace the nonfunctional enzymes in metabolically active regions of the lens. Without the ability to mount this response, aged lenses become deficient in GSH while other aged tissues remain abundant in the antioxidant. However, no direct measurement of Nrf2 was made in this study. Furthermore, since Nrf2 activation is regulated by binding events and PTMs,[20] it is premature to exclude a role for Nrf2 in lens adaptation to GSH-deficiency until such measurements are made.

Rather than a traditional oxidative stress response, the primary defensive adaptation that the lens shows at the transcript level is the upregulation of a multitude of detoxifying genes that may be able to carry out many of the same functions as GSH. The most robust response appears to be upregulation of the MTs, which are small cysteine-rich cytosolic proteins. Traditionally, MTs are thought of as heavy metal chelators but, more recently, they have been shown to be effective free radical scavengers[26] due to their abundance of free sulfhydryl residues. Both of these functions overlap with those of GSH[2] and indicate that MTs may be a highly effective substitute for GSH in regards to its nonenzymatic functions. In fact, studies have shown that a reduction in GSH results in upregulation of MT[27] and vice versa,[28] indicating a linkage between the two cytosolic pools. Additionally, regulation changes in MT have been noted in human cataractous

Investigative Ophthalmology & Visual Science

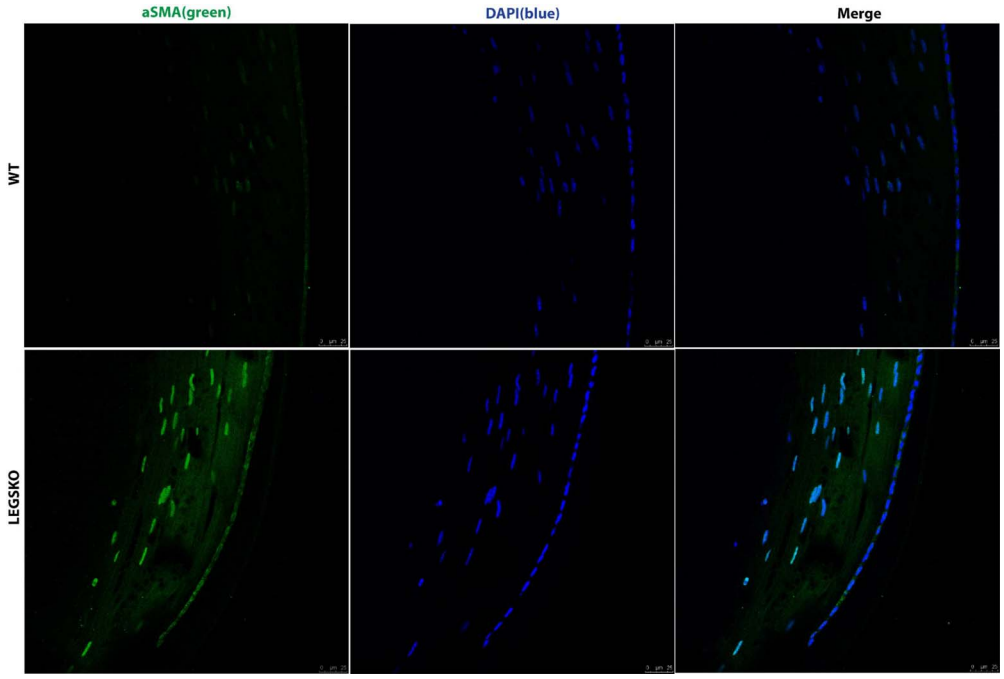

Figure 10. Immunofluorescent imaging of α-SMA in the GSH-deficient mouse lens. *Green* = α-SMA, *blue* = DAPI (nuclear stain).

lenses[29,30] and other mouse cataract models,[31] giving it a strong potential for protecting the lens.

Intriguingly, Western blot data (Fig. 9) indicate that MT is upregulated in the LEGSKO lens but downregulated by treatment with BSO. The reason for this discrepancy is unclear, especially when considering that the other measured protein changes were more robust in the BSO-treated lenses compared to the untreated lenses. One possibility is that the lens receives a large portion of its cytosolic cysteine via the γ-glutamyl cycle by the breakdown GSH in the surrounding fluids.[32] In this case, the systemic GSH-deficiency induced by BSO treatment leads to cysteine deficiency in the lens and thus a decrease in production of the cysteine-rich MT, but this does not occur in the untreated LEGSKO lens, which has a highly localized GSH-deficiency.

One of the major roles of GSH in the lens is the detoxification of toxic aldehydes, such as 4-hydroxynonenal, that result from lipid peroxidation,[33] a major consequence of UV irradiation.[34] GSH acts as a cofactor for glutathione-S-transferases (GST) to detoxify these molecules[35] and prevent damage to lenticular proteins. With GSH-deficiency, lenses show upregulation of four aldehyde dehydrogenases, *Aldh1a1*, *Aldh1a7*, *Aldh1l1*, and *Aldh3a1*, as well as the aldo-keto reductase *Akr1b10*, which can also detoxify aldehydes. Interestingly, *Aldh1a3* was slightly downregulated. *Aldh1a1* and *Aldh3a1* have previously been shown to be expressed in lenses at the protein level,[36] with ALDH1A1 being one of the major noncrystallin proteins of the lens,[37] and knockout of these groups leads to cataract formation.[36,38] ALDH1A7 is nearly identical in sequence to ALDH1A1 and has expectantly similar function and substrate affinity.[39] *Aldh1l1* encodes 10-formyltetrahydrofolate dehydrogenase so this gene does not play the same role in the detoxification of aldehydes as its other family members. *Aldh1a3* is involved in both eye development and retinal metabolism,[40] so its downregulation is consistent with the trend of other vision genes found in the lens GSH-deficient transcriptome. Aldose reductase has been found to be important in the formation of diabetic cataract,[41] but studies indicate that AKR1B10 does not contribute to this pathology.[42] Thus, the upregulation of *Akr1b10* found here most likely relates to its ability to detoxify lipid peroxidation products and is a protective adaptation.

Carboxylesterase hydrolyzes toxic carboxylic esters, many of which can also be detoxified by GSTs, and has a known expression in the lens,[43] so its upregulation in the GSH-deficient transcriptome has a potentially protective role. Interestingly, it has been found that carboxylesterase activity in the lens decreases steadily with age due to glycation of the enzyme,[44] indicating a possible role in human cataract.

Little inquiry into urea transport in the lens has been made, but production of urea and other nitrogenous waste products has been demonstrated in the lens.[45] The robust upregulation of urea efflux transporter UT-B, encoded by *Slc14a1*, found in the GSH-deficient lens transcriptome could mean that detoxification of nitrogenous waste products is an important function of GSH in the lens and that, in the absence of GSH, export of these groups is essential. It has been demonstrated in vivo that lens crystallins are susceptible to carbamylation when subjected to cyanate, a urea derivative.[46] In preliminary experiments, we find that urea export is highly elevated in LEGSKO lenses (data not shown).

AS3MT detoxifies the oxidative group arsenite. Arsenite has been shown to accumulate significantly in the lens[47] and GSH has been reported as an effective reductant for AS3MT-catalyzed reactions,[48] so its upregulation appears to be protective and it could play a currently uncharacterized role in lenticular homeostasis.

The GSH-Deficient Lens Shows Numerous Changes in Transport Systems

Due to its avascular nature and the lack of metabolic machinery throughout much of the lens, transport processes are essential to the function of the lens.[49] The lens relies on both gap junctional coupling and a microcirculation induced by Na^+/K^+ currents in order to ensure that all lens cells receive nutrients. Major changes were seen in several different groups

of transporters and transport-related genes in the GSH-deficient lens transcriptome.

Lenses are thought to exclusively express Cx43, Cx46, and Cx50 connexins at the protein level,[50] so it is unclear whether the upregulation of *Gjb3* (Cx31), and the less robust downregulation of *Gjb6* (Cx30; Supplementary Data), have any actual impact on the lens. Inappropriate expression of connexins could lead to dysfunction, and thus cataract, in the lens. However, it should be noted that, even at their highest expression level, the RPKM values of these transcripts are at least 500-fold less than the characterized lens connexin genes.

In addition to upregulation of *Kcnd1*, other ion channel gene changes with a potential role in lenticular microcirculation, such as *Kcnd3, Kcnj13, Kcnip1,* and *Scnn1b* (Supplementary Data), were noted but the end result is unclear since there was a mix of up- and downregulation in these genes and the net effect on ion flow cannot be determined.

One transport system with a change in a clear direction is iron transport, which showed robust upregulation of the iron uptake proteins *Trf* and *Snca*, as well as a slight upregulation of ferrireductase *Steap3* and downregulation of the iron exporter *Slc40a1* (Supplementary Data). The reason for this change is unclear, but it indicates that GSH-deficient lenses have enhanced uptake and retention of iron. Because free iron can induce the Fenton reaction,[51] increased lenticular iron could be a major danger to lens protein. One possible explanation for this seemingly paradoxical adaptation is that GSH-deficiency, including deficiency induced by BSO treatment, has been shown to induce ferroptosis, a form of programmed cell death independent from apoptosis.[52] This pathway relies on iron accumulation and oxidative stress, rather than caspase activation, to kill cells. Given the total lack of changes seen in apoptotic genes, despite the cells being under oxidative stress conditions, this data could mean that ferroptosis is potentially the primary mode of programmed cell death in the lens. If this pathway is truly being activated in the lens, it could have a major impact on lens health and clarity. Iron accumulation has been noted in cataractous human lenses,[53] indicating a relationship between these results and human disease.

There were also several changes in γ-aminobutyric acid (GABA) receptors. Expression of GABA receptors has previously been characterized in the lens and it is believed that these proteins play a role in fiber differentiation since they can be found in abundance at the tips of elongating fiber cells but not in mature differentiated fiber cells.[54] The large regulation changes in GABA receptors found in the GSH-deficient lens transcriptome could disrupt proper fiber cell differentiation and, thus lens clarity, and may relate to a potential dysfunction in differentiation discussed elsewhere in this paper.

GSH-Deficient Lenses Have Altered Lipid Metabolism

Lipid metabolism is essential to lens clarity for several reasons. Lens cell membranes have among the highest concentration of cholesterol of any tissue in the body.[55] A major reason for this adaptation is that cholesterol-rich membranes are less permeable to O_2, which is not needed in the mitochondrial-free regions of the lens and can potentially lead to protein oxidation. This membrane composition produces an O_2-depleted environment, with minimal levels of O_2 present in the lens nucleus.[55] Additionally, it has recently been found that sterols have a direct role in preventing aggregation of lens proteins and that 25-hydroxycholesterol[56] and lanosterol[57] treatment can even reverse lens protein aggregation in vivo. Further evidence for the importance of cholesterol metabolism in the lens is demonstrated by the fact that the use of cholesterol-lowering statin drugs significantly increases the risk of cataract development.[58]

Abca1 and *Apoe* were both upregulated in fiber cells (Supplementary Data) and are known to work together to export cholesterol from cells.[59] The related transporters *Abca13* and *Abcg1* were also upregulated in fiber cells and may be involved in this process. At the same time, other changes indicate changes to the uptake of lipids, as evidenced by the upregulation of lipoprotein lipase and downregulation of lipase inhibitors *Plin4* and *Plin5* (Supplementary Data), indicating enhanced uptake of lipids. However, lipase inhibitor *G0s2* (Fig. 6) and *Pcsk9* (Supplementary Data), which induces degradation of LDL receptor,[60] were upregulated and the fatty acid importer *Cd36* was downregulated (Supplementary Data), indicating depressed uptake of lipids. Thus, the end result of these regulation changes is somewhat unclear but any change to lens membrane composition or sterol synthesis could have a major effect on lens clarity. The lipid content of lenses will need to be investigated further to determine how these regulation changes affect cataractogenesis and how they relate to GSH-deficiency.

GSH-Deficient Lenses Show Activation of EMT Signaling and a Loss of Differentiation

Posterior capsular opacification (PCO), also known as secondary cataract, is a major consequence of cataract surgery.[61] PCO occurs when residual lens epithelia left on the lens capsule after surgery proliferate, migrating to the posterior lens capsule, and undergo EMT, forming fibrotic lesions that prevent focusing of light onto the retina.[61] Thus, understanding factors that govern lens EMT is essential to reducing the incidence of PCO.

We were surprised to find robust EMT-related transcriptional changes in the epithelia of GSH-deficient lenses. This response is evidenced by the top upstream regulators of the transcriptomic changes being EMT-regulators including TGF-β1, TNF, and p53 (Table 1) and by the upregulation of genes involved in the activation of canonical EMT pathways, such as *Egf, Fgfr4, Wnt10a,* and *Il-1B* (Fig. 7A). While many downstream members of EMT signaling are governed by binding events, turnover, and PTMs, these activators of EMT signaling are primarily by mRNA levels. Accompanying the upregulation of these EMT initiators were changes indicative of an active EMT phenotype in lens epithelia, including an upregulation of histones that demonstrates cellular proliferation (Fig. 7C) and changes to ECM organization (Fig. 7D). BSO-treated lenses also showed a broad downregulation of genes associated with vision, which could be considered eye marker genes (Fig. 7B). This change seems to strongly indicate a loss of proper differentiation in GSH-deficient lens epithelia. This is supported by the decrease in β- and γ-crystallin expression (Fig. 3), which are restricted to lens tissue and thus highly specific markers. Interestingly, one exception to this trend was the slight upregulation of lens epithelia marker *Foxe3* (Supplementary Data). This gene encodes a transcription factor that is essential to lens development, but its activity induces proliferation of lens epithelia and inhibits the proper differentiation of lens fiber cells.[62] Thus, overexpression of *Foxe3* may promote inappropriate lens epithelia cell growth and disrupt lenticular morphology, contributing to EMT-mediated pathology.

In comparing the GSH-deficient lens transcriptome to the transcriptional profile of mouse lens epithelia actively undergoing EMT (Table 2), a major similarity was the loss of vision genes, including *Crybb1, Rho, Rbp3*, and *Lim2*, as well as changes in genes relating to lipid homeostasis, such as *Apoe, Ldlr,* and *Fabp5*, histone upregulation, and fibrotic changes

Investigative Ophthalmology & Visual Science

that include an upregulation of the EMT-related *Tnc*. These results show that the GSH-deficient mouse lens transcriptome recapitulates many of the same features of the EMT lens transcriptome.

While transcriptional changes imply that GSH-deficient lens epithelia are primed for EMT, true activation of EMT signaling was confirmed by analyzing the expression of several proteins involved in EMT. TNC, LAMB3, and type I collagen levels were measured by Western blot (Figs. 9F–H). In all cases, it was found that the proteins were upregulated in BSO-treated LEGSKO lens epithelia ($P < 0.05$) but not in untreated LEGSKO lens epithelia, consistent with the transcriptomic data, which show a more robust EMT-like transcriptional profile after BSO treatment. TNC, LAMB3, and type I collagen have all been shown to play a role in the fibrotic changes associated with EMT and are produced in response to activation of EMT signaling pathways.[63–65]

WNT10A, which appeared to be the major driver of lenticular EMT based on the transcriptional data (Fig. 7), was analyzed in the aqueous humor of these mice. WNT10A >3-fold upregulated in LEGSKO aqueous humor ($P < 0.05$) and >8-fold upregulated in BSO-treated LEGSKO aqueous humor ($P < 0.05$; Fig. 9I). This confirms the importance of WNT10A signaling in the lens and further demonstrates the more robust EMT response in the BSO-treated lens.

The expression of α-SMA, a widely used marker of EMT, was analyzed in GSH-deficient lenses by immunofluorescent imaging (Fig. 10). GSH-deficient lenses showed a greatly enhanced expression of α-SMA, although disrupted morphology is not evident in these images.

Analogies and Differences From Other Models of Oxidative Stress and GSH-Depletion

One important question is the extent to which the above findings serve as a blue print for genetic response to oxidative stress in other systems. While a strong relationship exists between low GSH and oxidative stress, the reverse is not necessarily true. One gene expression study on the response of the human lens epithelial cell line SRA 01-04 to acute H_2O_2 exposure[66] found differential gene expression of glutamine cyclotransferase (*Qpct*), cytokine inducible nuclear protein (*Cinp*), glycoprotein 130 (*Gp130*), ribosomal protein S10 (*Rps10*), mitochondrial NADH dehydrogenase 4 (*Mt-Nd4*), mitochondrial NADH dehydrogenase 5 (*Mt-Nd5*), mitochondrial cytochrome b (*Mt-Cyb*), mitochondrial 16S rRNA (*Mt-Rnr2*), cathepsin (*Cst*), alternative splicing factor (*Asf*), and β-hydroxyisobutyryl-coenzyme A hydrolase (*Hibch*). These specific gene changes do not have any overlap with the data presented in this paper and primarily relate to a downregulation in mitochondrial activity, likely as a means to reduce production of oxidative species. However, the authors do note that some of these changes, such as upregulation of *Asf* and *Cinp* are associated with epithelial cancers and regulated by TNF, indicating some similarity in signaling.

Another study determined differentially regulated genes in the mouse lens epithelial cell line αTN4 after chronic H_2O_2 exposure.[67] This study found upregulation of catalase (*Cat*), glutathione peroxidase (*Gpx*), ferritin light chain (*Ftl*), ferritin heavy chain (*Fth1*), reticulocalbin (*Rcn1*), and *Cryab*, and downregulation of *Cryaa*. This study reported a lack of change in mitochondrial genes and in *Mt2*. Once again, there was a lack of specific overlap in these results, which show a more traditional oxidative stress response, and what we found in GSH-depleted lenses. However, changes in iron homeostasis and binding are indicated by the upregulation of ferritin, similar to how GSH-depleted lenses show an upregulation in *Trf* and other iron homeostasis genes. Additionally, the downregulation of *Cryaa* is similar to the downregulation of crystallins and other eye genes found in the GSH-depleted lens and also indicates a possible movement of the cells away from their proper lineage. No studies on gene expression responses to oxidative stress in lens fiber cells exist for comparison to our data.

Looking more generally at global transcriptomic responses to oxidative stress outside of the lens, one study treated cultured bovine blastocysts with either the pro-oxidant 0.01 mM 2,2′-azobis (2-amidinopropane) dihydrochloride (AAPH) or BSO and measured the response using microarrays.[68] This study found that of the 231 gene changes in AAPH-treated blastocysts and 481 gene changes in BSO-treated blastocysts, 69 of the gene changes overlapped. This demonstrates that GSH-depletion causes many changes outside of traditional oxidative stress responses and may not induce many expected oxidative stress responses, as we have shown in this study. Interestingly, the transcriptomic profile of AAPH-treated blastocysts, which showed TGF-β and TNF signaling and ECM organization as top altered pathways and changes in *Col1a2, Dcn,* and *Serpine1*, was more similar to that of GSH-depleted lenses than that of BSO-treated blastocysts, which instead showed a traditional Nrf2-mediated response.

There are a number of possible reasons for the differences between other studies and our results. One reason is that GSH-depletion alone may not truly induce oxidative stress in the lens, which exists in an oxygen-depleted environment with a low amount of metabolic activity, which is in direct contrast to cultured cell lines and blastocysts, which are rapidly dividing and exposed to much higher levels of oxygen. Another is that GSH, which can be conjugated to a multitude of proteins and other compounds, has many effects outside of antioxidant defense pathways. The differences and similarities between this study and others indicates that culture systems and treating lenses with high levels of pro-oxidants may not be accurate methods to model the environment of the aging lens.

Limitations of This Study

The data presented above represent a comprehensive picture of the genetic response by the lens to GSH depletion. However, the degree to which the changes noted here are carried through to the protein level remains largely unknown. Protein expression for a subset of genes was tested and was found to correlate with the transcriptomic data (Fig. 9). In general, the response at the protein level appeared more muted than at the transcriptional level, with smaller fold changes and some changes only present in the BSO-treated LEGSKO lens. The unexpected downregulation of MTs in the BSO-treated LEGSKO lens highlights the fact that protein expression is not solely governed by mRNA levels and other factors may play an equal or more important role in many cases. Thus, in order to further confirm the transcriptomic data and determine additional changes not found at the transcript level, a follow-up proteomics study is in progress. This study will examine the extent to which the observed genetic changes result in translational changes and any differences between the GSH-depleted lens transcriptome and proteome.

Conclusions

The GSH-deficient mouse lens transcriptome shows significant changes in lipid homeostasis, transport systems, and detoxifying genes, as well as a clear activation of EMT signaling. Protein expression data confirm that many of these changes are present at the protein level, though likely to a lesser degree, and that EMT signaling is activated. This data give new insights

Investigative Ophthalmology & Visual Science

into cellular adaptation to and consequences of GSH-deficiency and show that lenses may not mount a typical oxidative stress response to GSH depletion. It also indicates GSH as an important mediator of EMT-related pathology in the lens.

Acknowledgments

Supported by Grants EY07099 (VMM), EY024553 (XF), T32 EY007157 to the Visual Sciences Research Center at Case Western Reserve University, and T32 EY024236 to the Cole Eye Institute at the Cleveland Clinic.

Disclosure: **J.A. Whitson**, None; **X. Zhang**, None; **M. Medvedovic**, None; **J. Chen**, None; **Z. Wei**, None; **V.M. Monnier**, None; **X. Fan**, None

References

1. Petrash JM. Aging and age-related diseases of the ocular lens and vitreous body. *Invest Ophthalmol Vis Sci*. 2013;54:54–59.
2. Giblin FJ. Glutathione: a vital lens antioxidant. *J Ocul Pharmacol Ther*. 2000;16:121–135.
3. Rathbun WB, Schmidt AJ, Holleschau AM. Activity loss of glutathione synthesis enzymes associated with human subcapsular cataract. *Invest Ophthalmol Vis Sci*. 1993;34:2049–2054.
4. Sweeney MH, Truscott RJ. An impediment to glutathione diffusion in older normal human lenses: a possible precondition for nuclear cataract. *Exp Eye Res*. 1998;67:587–595.
5. Fan X, Liu X, Hao S, Wang B, Robinson ML, Monnier VM. The LEGSKO mouse: a mouse model of age-related nuclear cataract based on genetic suppression of lens glutathione synthesis. *PLoS One*. 2012;7:e50832.
6. Whitson JA, Sell DR, Goodman MC, Monnier VM, Fan X. Evidence of dual mechanisms of glutathione uptake in the rodent lens: a novel role for vitreous humor in lens glutathione homeostasis. *Invest Ophthalmol Vis Sci*. 2016;57:3914–3925.
7. Ohrloff C, Hockwin O. Lens metabolism and aging: enzyme activities and enzyme alterations in lenses of different species during the process of aging. *J Gerontol*. 1983;38:271–277.
8. Hoang TV, Kumar PK, Sutharzan S, Tsonis PA, Liang C, Robinson ML. Comparative transcriptome analysis of epithelial and fiber cells in newborn mouse lenses with RNA sequencing. *Mol Vis*. 2014;20:1491–1517.
9. Termén S, Tan EJ, Heldin CH, Moustakas A. p53 regulates epithelial-mesenchymal transition induced by transforming growth factor β. *J Cell Physiol*. 2013;228:801–813.
10. Davies P, Moualla D, Brown DR. Alpha-synuclein is a cellular ferrireductase. *PLoS One*. 2011;6:e15814.
11. Cao CY, Mok SW, Cheng VW, Tsui SK. The FHL2 regulation in the transcriptional circuitry of human cancers. *Gene*. 2015;572:1–7.
12. Barson JR, Morganstern I, Leibowitz SF. Galanin and consummatory behavior: special relationship with dietary fat, alcohol and circulating lipids. *EXS*. 2010;102:87–111.
13. Medici D, Nawshad A. Type I collagen promotes epithelial-mesenchymal transition through ILK-dependent activation of NF-kappaB and LEF-1. *Matrix Biol*. 2010;29:161–165.
14. Danysh BP, Duncan MK. The lens capsule. *Exp Eye Res*. 2009;88:151–164.
15. Jensen MA, Wilkinson JE, Krainer AR. Splicing factor SRSF6 promotes hyperplasia of sensitized skin. *Nat Struct Mol Biol*. 2014;21:189–197.
16. Järvinen TAH, Prince S. Decorin: a growth factor antagonist for tumor growth inhibition. *BioMed Res Internat*. 2015;2015:654765.
17. Norose K, Clark JI, Syed NA, et al. SPARC deficiency leads to early-onset cataractogenesis. *Invest Ophthalmol Vis Sci*. 1998;39:2674–2680.
18. Medvedovic M, Tomlinson CR, Call MK, Grogg M, Tsonis PA. Gene expression and discovery during lens regeneration in mouse: regulation of epithelial to mesenchymal transition and lens differentiation. *Mol Vis*. 2006;12:422–440.
19. Fan X, Zhou S, Wang B, et al. Evidence of highly conserved β-crystallin disulfidome that can be mimicked by in vitro oxidation in age-related human cataract and glutathione depleted mouse lens. *Mol Cell Proteomics*. 2015;14:3211–3223.
20. Ma Q. Role of Nrf2 in oxidative stress and toxicity. *An Rev Pharmacol Toxicol*. 2013;53:401–426.
21. He X, Ma Q. Redox regulation by nuclear factor erythroid 2-related factor 2: gatekeeping for the basal and diabetes-induced expression of thioredoxin-interacting protein. *Mol Pharmacol*. 2012;82:887–897.
22. Wu KC, Cui JY, Klaassen CD. Effect of graded Nrf2 activation on phase-I and -II drug metabolizing enzymes and transporters in mouse liver. *PLoS One*. 2012;7:e39006.
23. Nebert DW, Vasiliou V. Analysis of the glutathione S-transferase (GST) gene family. *Hum Genomics*. 2004;1:460–464.
24. Li J, Xia Z, Ding J. Thioredoxin-like domain of human κ class glutathione transferase reveals sequence homology and structure similarity to the θ class enzyme. *Protein Sci*. 2005;14:2361–2369.
25. Liu M, Chen H, Wei L, et al. Endoplasmic reticulum (ER) localization is critical for DsbA-L protein to suppress ER stress and adiponectin down-regulation in adipocytes. *J Biol Chem*. 2015;290:10143–10148.
26. Viarengo A, Burlando B, Ceratto N, Panfoli I. Antioxidant role of metallothioneins: a comparative overview. *Cell Mol Biol*. 2000;46:407–417.
27. Ding HQ, Zhou BJ, Liu L, Cheng S. Oxidative stress and metallothionein expression in the liver of rats with severe thermal injury. *Burns*. 2002;28:215–221.
28. Hidalgo J, Garvey JS, Armario A. On the metallothionein, glutathione and cysteine relationship in rat liver. *J Pharmacol Exp Ther*. 1990;255:554–564.
29. Hawse JR, Hejtmancik JF, Horwitz J, Kantorow M. Identification and functional clustering of global gene expression differences between age-related cataract and clear human lenses and aged human lenses. *Exp Eye Res*. 2004;79:935–940.
30. Ruotolo R, Grassi F, Percudani R, et al. Gene expression profiling in human age-related nuclear cataract. *Mol Vis*. 2003;9:538–548.
31. Mansergh FC, Wride MA, Walker VE, Adams S, Hunter SM, Evans MJ. Gene expression changes during cataract progression in Sparc null mice: differential regulation of mouse globins in the lens. *Mol Vis*. 2004;10:490–511.
32. Said R, Bonne C, Regnault F, Sincholle D. In vitro study of gamma-glutamyl transpeptidase in rat lens. *Exp Eye Res*. 1983;37:273–278.
33. Micelli-Ferrari T, Vendemiale G, Grattagliano I, et al. Role of lipid peroxidation in the pathogenesis of myopic and senile cataract. *Br J Ophthalmol*. 1996;80:840–843.
34. van Kuijk FJ. Effects of ultraviolet light on the eye: role of protective glasses. *Environ Health Perspect*. 1991;96:177–184.
35. Singhal SS, Singh SP, Singhal P, Horne D, Singhal J, Awasthi S. Antioxidant role of glutathione S-transferases: 4-Hydroxynonenal, a key molecule in stress-mediated signaling. *Toxicol Appl Pharmacol*. 2015;289:361–370.
36. Choudhary S, Xiao T, Vergara LA, et al. Role of aldehyde dehydrogenase isozymes in the defense of rat lens and human

lens epithelial cells against oxidative stress. *Invest Ophthalmol Vis Sci*. 2005;46:259–267.

37. Chen Y, Koppaka V, Thompson DC, Vasiliou V. ALDH1A1: from lens and corneal crystallin to stem cell marker. *Exp Eye Res*. 2012;102C:105–106.
38. Lassen N, Bateman JB, Estey T, et al. Multiple and additive functions of ALDH3A1 and ALDH1A1: cataract phenotype and ocular oxidative damage in Aldh3a1(-/-)/Aldh1a1(-/-) knockout mice. *J Biol Chem*. 2007;282:25668–25676.
39. Black WJ, Stagos D, Marchitti SA, et al. Human aldehyde dehydrogenase genes: alternatively-spliced transcriptional variants and their suggested nomenclature. *Pharmaco Genomics*. 2009;19:893–902.
40. Molotkov A, Molotkova N, Duester G. Retinoic acid guides eye morphogenetic movements via paracrine signaling but is unnecessary for retinal dorsoventral patterning. *Development*. 2006;133:1901–1910.
41. Snow A, Shieh B, Chang KC, et al. Aldose reductase expression as a risk factor for cataract. *Chem Biol Interact*. 2015;234:247–253.
42. Huang SP, Palla S, Ruzycki P, et al. Aldo-Keto reductases in the eye. *J Ophthalmol*. 2010;2010:521204.
43. Sanghani SP, Sanghani PC, Schiel MA, Bosron WF. Human carboxylesterases: an update on CES1, CES2 and CES3. *Protein Pept Lett*. 2009;16:1207–1214.
44. Yan H, Harding JJ. Carnosine protects against the inactivation of esterase induced by glycation and a steroid. *Biochim Biophys Acta*. 2005;1741:120–126.
45. Jernigan HM Jr. Urea formation in rat, bovine, and human lens. *Exp Eye Res*. 1983;37:551–558.
46. Yan H, Zhang J, Harding JJ. Identification of the preferentially targeted proteins by carbamylation during whole lens incubation by using radio-labelled potassium cyanate and mass spectrometry. *Int J Ophthalmol*. 2010;3:104–111.
47. Kleiman NJ, Quinn AM, Fields KG, Slavkovich V, Graziano JH. Arsenite accumulation in the mouse eye. *J Toxicol Environ Health A*. 2016;79:339–341.
48. Dheeman DS, Packianathan C, Pillai JK, Rosen BP. Pathway of human AS3MT arsenic methylation. *Chem Res Toxicol*. 2014;27:1979–1989.
49. Donaldson P, Kistler J, Mathias RT. Molecular solutions to mammalian lens transparency. *News Physiol Sci*. 2001;16:118–123.
50. Mathias RT, White TW, Gong X. Lens gap junctions in growth, differentiation, and homeostasis. *Physiol Rev*. 2010;90:179–206.
51. Winterbourn CC. Toxicity of iron and hydrogen peroxide: the Fenton reaction. *Toxicol Lett*. 1995;82–83:969–974.
52. Yu H, Guo P, Xie X, Wang Y, Chen G. Ferroptosis, a new form of cell death, and its relationships with tumorous diseases. *J Cell Mol Med*. 2017;21:648–657.
53. Dawczynski J, Blum M, Winnefeld K, Strobel J. Increased content of zinc and iron in human cataractous lenses. *Biol Trace Elem Res*. 2002;90:15–23.
54. Frederikse PH, Kasinathan C. Lens GABA receptors are a target of GABA-related agonists that mitigate experimental myopia. *Med Hypotheses*. 2015;84:589–592.
55. Subczynski WK, Raguz M, Widomska J, Mainali L, Konovalov A. Functions of cholesterol and the cholesterol bilayer domain specific to the fiber-cell plasma membrane of the eye lens. *J Membr Biol*. 2012;245:51–68.
56. Makley LN, McMenimen KA, DeVree BT, et al. Pharmacological chaperone for α-crystallin partially restores transparency in cataract models. *Science*. 2015;350:674–677.
57. Zhao L, Chen XJ, Zhu J, et al. Lanosterol reverses protein aggregation in cataracts. *Nature*. 2015;523:607–611.
58. Wise SJ, Nathoo NA, Etminan M, Mikelberg FS, Mancini GB. Statin use and risk for cataract: a nested case-control study of 2 populations in Canada and the United States. *Can J Cardiol*. 2014;30:1613–1619.
59. Getz GS, Reardon CA. Apoprotein E as a lipid transport and signaling protein in the blood, liver, and artery wall. *J Lipid Res*. 2009;50:S156–S161.
60. Lagace TA. PCSK9 and LDLR degradation: regulatory mechanisms in circulation and in cells. *Curr Opin Lipidol*. 2014;25:387–393.
61. Wormstone IM, Wang L, Liu CS. Posterior capsule opacification. *Exp Eye Res*. 2009;88:257–269.
62. Landgren H, Blixt A, Carlsson P. Persistent FoxE3 expression blocks cytoskeletal remodeling and organelle degradation during lens fiber differentiation. *Invest Ophthalmol Vis Sci*. 2008;49:4269–4277.
63. Tanaka S, Sumioka T, Fujita N, et al. Suppression of injury-induced epithelial-mesenchymal transition in a mouse lens epithelium lacking tenascin-C. *Mol Vis*. 2010;16:1194–1205.
64. Wang XM, Li J, Yan MX, et al. Integrative analyses identify osteopontin, LAMB3 and ITGB1 as critical pro-metastatic genes for lung cancer. *PLoS One*. 2013;8:e55714.
65. Medici D, Nawshad A. Type I collagen promotes epithelial-mesenchymal transition through ILK-dependent activation of NF-kappaB and LEF-1. *Matrix Biol*. 2010;29:161–165.
66. Carper DA, Sun JK, Iwata T, et al. Oxidative stress induces differential gene expression in a human lens epithelial cell line. *Invest Ophthalmol Vis Sci*. 1999;40:400–406.
67. Carper D, John M, Chen Z, et al. Gene expression analysis of an H(2)O(2)-resistant lens epithelial cell line. *Free Radic Biol Med*. 2001;31:90–97.
68. Cagnone GL, Sirard MA. Transcriptomic signature to oxidative stress exposure at the time of embryonic genome activation in bovine blastocysts. *Mol Reprod Dev*. 2013;80:297–314.

Investigative Ophthalmology & Visual Science